# Spectral Approximation of Navier-Stokes Equations

**Chapter** · July 2011

DOI: 10.1007/978-3-0348-8424-2_2

CITATIONS
4

READS
438

**3 authors**, including:

Paola Gervasio
Università degli Studi di Brescia
**127** PUBLICATIONS **588** CITATIONS
SEE PROFILE

Alfio Quarteroni
Politecnico di Milano
**881** PUBLICATIONS **32,344** CITATIONS
SEE PROFILE

# Spectral Approximation of Navier-Stokes Equations*

P. Gervasio†, A. Quarteroni‡ and F. Saleri§

**Abstract**

We review some basic aspects of spectral methods and their application to the numerical solution of Navier-Stokes equations for viscous incompressible flows.

## Introduction

Spectral methods are today widely used for the approximation of partial differential equations. They are intrinsically very accurate, and they become computationally effective also for non cartesian domains, provided they are used in a domain decomposition framework in which case the domain is split into subdomains that can be mapped into a reference square (or cube). The spectral element method provides an instance of domain decomposition approach.
Spectral methods were initially used for the approximation of differential problems with periodic boundary conditions, with a Galerkin approach and Fourier basis functions. In 1965 the introduction of the FFT algorithm, that allows to *travel* from the physical space and the frequency space by $\mathcal{O}(N \log_2 N)$ floating point operations versus $\mathcal{O}(N^2)$ that would be required otherwise (say using a matrix-vector product), gave a great impulse to the development of the method.
Earliest theoretical results, concerning stability and convergence of spectral methods are due to Gottlieb and Orszag.
Afterwards, in the seventhies, spectral methods have been extended to differential problems with non periodic boundary conditions, by the use of Chebyshev and Legendre systems, for two- and three-dimensional domains. The first estimates of the approximation errors in Sobolev norms, obtained by functional analysis arguments, are due to Canuto and Quarteroni (see [19]).
From the computational viewpoint, the use of a tensorial basis has limited this type of methods to tensorial shaped domains (i.e. deformations of parallelotop domains) until spectral methods were adapted to domains with more general geometries in the eighties: Patera introduced spectral elements ([62], [51]), Morchoisne proposed the overlapping domain decomposition methods ([56]) and Quarteroni the

*This research has been carried out with the support of M.U.R.S.T. through "Fondi 40%" and C.N.R. "Prog. Speciale Fluidodinamica e Dinamica Molecolare".

†Department of Mathematics, University of Brescia, Brescia (Italy)
‡Department of Mathematics, Politecnico of Milano, Milano (Italy) and EPFL, Lausanne (CH)
§Department of Mathematics, University of Milano, Milano (Italy)

non-overlapping domain decomposition methods ([68]).
An historical account on the "early stage" of spectral methods is given e.g. in the books [36], [16], [10].

Since their origin spectral methods were applied to the mechanics of viscous incompressible flows. This paper pays special attention to the approximation of the Navier Stokes equations in the primitive variable formulation. In this case, the velocity and the pressure cannot be chosen independently; indeed, a compatibility condition (the so-called Ladyzenskaya-Brezzi-Babuška or inf-sup condition) has to be satisfied in order to avoid spurious modes on the pressure. Moreover, for the Navier Stokes equations for high Reynolds number flows, the dominating convection terms produce another type of instability that generates oscillations on the velocity field.
In the spectral context, the most widely used method to avoid the spurious modes on the pressure is the so called $(\mathbb{Q}_N - \mathbb{Q}_{N-2})$ approach. It was proposed by Maday, Meiron, Patera and Ronquist ([50]) and it consists of choosing the space of polynomials of degree $N$ (in each variable) for the velocity and of degree $N-2$ for the pressure. The LBB condition id satisfied with a constant $\beta$ which behaves like $N^{-1/2}$. Another approach, which is less used, consists in using polynomials with the same degree for both the velocity and the pressure with a-posteriori filtering of parasitic modes for the pressure ([5]).
Otherwise, one has to relax the incompressibility condition, in which case the LBB condition doesn't necessarily have to be fulfilled. An example is provided by the adaption to the spectral context (see [34], [17]) of the stabilization techniques that have been originally proposed for the finite element approximation of the Stokes problem (see Brezzi and Pitkaranta [13] and Hughes, Franca and Balestra [39]) and of the incompressible Navier-Stokes equations (see Brooks and Hughes [14] and Franca and Frey [30]).

About the approximation of the time-dependent Navier-Stokes equations we give an account of those numerical methods which can be defined through a separation between temporal and spatial discretization. We deal with semi-implicit finite-difference and fractional step schemes, largely used in the spectral framework. The former avoid the resolution of non-linear systems (contrary to implicit methods) and retain reasonably good stability properties.
The latter are based on the splitting of the differential operator in two or more suboperators such that the original problem can be reduced to the subsequent resolution of simpler differential problems (such as elliptic or Stokes equations). Inside the spectral method context the fractional step schemes (and, in particular, the projection methods) have been used, among others, by Shen ([77]), Pinelli et al. ([66]), Karniadakis et al. ([42]). Splitting methods using Adams-Bashforth or Adams-Moulton multistep schemes were considered by Karniadakis et al. ([42]), Orszag and Kells ([57]) and Marcus ([53]). Operator factor splitting was considered by Maday, Patera and Ronquist ([52]).
We observe that, with the exception of the stabilized approach, all the previous schemes lead to the successive resolution of subproblems that may be either elliptic problems (linear or non linear) or a generalized form of the Stokes problem. Therefore, in order to achieve an overall globally efficient algorithm, it is mandatory to tackle effectively these computational kernels.

Domain decomposition methods offer a chance in this respect. We review here the domain decomposition formulation of linear elliptic, generalized Stokes and Navier-Stokes problems. In particular, on the Poisson problem we describe different iterative procedure to implement the domain decomposition techniques: the classical iterative substructuring methods such as Dirichlet-Neumann ([68]), Neumann-Neumann ([9]) and Robin ([48]); and the projection decomposition method associated to spectral collocation ([33]). A brief review on the overlapping Schwarz method is done in connection with the method proposed by Pavarino ([63]) (see also Pahl ([60]) and Casarin ([21])).
The Dirichlet-Neumann scheme is also presented for the Stokes problem, while the Navier-Stokes equations are discretized by stabilized spectral elements. The paper ends with some numerical results obtained by the stabilized spectral element approximation of the Navier-Stokes system, which are obtained by the BiCGStab iterations preconditioned by the finite element matrices.

# 1 Mathematical foundation and different paradigms of spectral methods

Spectral methods are among the most commonly used methods for the approximation of partial differential equations. Historically, spectral methods have been associated with Fourier expansion and they have been applied to approximate periodic functions. However, nowadays they are used indifferently for periodic as well as general boundary-value problems. For the latter, algebraic polynomial expansions (especially Chebyshev's and Legendre's) are used in lieu of Fourier trigonometric polynomials.

The basic idea behind the classical single-domain spectral approach consists of approximating the solution of a differential problem, $u \in W$, by an infinitely differentiable function $u_N \in W_N$, with $W_N$ a subspace of $W$. The function $u_N$ is a trigonometric polynomial in the Fourier approach or an algebraic polynomial in the Legendre or Chebyshev system. It follows that the accuracy of the approximation is inherently high and actually depends solely on the regularity of the exact solution.

The discrete spectral problem is obtained by the projection of the differential equations to be solved on a finite dimensional space $V_N$ (possibly coinciding with $W_N$) by a suitable projection operator $P_N$ and, if $W_N \neq V_N$, it is required that $\dim V_N \equiv \dim W_N$. We refer to $W_N$ and $V_N$ as the space of the trial and test functions, respectively. The choice of $\{P_N,\ W_N,\ V_N\}$ characterises completely the type of spectral approximation. Three different spectral schemes, *Galerkin, tau* and *collocation*, are typically used.

The Galerkin and collocation schemes can be applicable to the Fourier or the algebraic approximation, on the contrary the tau approach is applicable solely to problems with non-periodic boundary conditions.

In order to briefly describe the spectral schemes we consider the following linear differential problem:

$$\begin{cases} Lu = f & \text{in } \Omega, \\ Bu = 0 & \text{on } \partial\Omega, \end{cases} \tag{1}$$

where $\Omega$ is an open bounded domain in $\mathbb{R}^d$ ($d = 1, 2, 3$) of boundary $\partial\Omega$, $L$ is a linear differential operator, $B$ is a set of linear boundary differential operators on $\partial\Omega$ and $f$ a suitable function in $L^2(\Omega)$. The corresponding variational formulation reads:

$$\text{find } u \in W : \ a(u, v) = \mathcal{F}(v) \qquad \forall v \in V, \tag{2}$$

where $a : W \times V \to \mathbb{R}$ is the bilinear form associated to $L$ and $\mathcal{F}$ is a linear continuous functional associated to $f$ and to the boundary differential operator $B$.

The *Galerkin* approach is characterised by choosing the same space for the test and trial functions (i.e. $W_N = V_N$) and $P_N$ as the classical $L^2(\Omega)$ projection operator from $V$ to $V_N$, i.e.

$$(P_N u, v_N)_{L^2(\Omega)} = (u, v_N)_{L^2(\Omega)}, \qquad \forall v_N \in V_N. \tag{3}$$

The Galerkin approximation to (2) reads:

$$\text{find } u_N \in V_N : \ a(u_N, v_N) = \mathcal{F}(v_N) \qquad \forall v_N \in V_N. \tag{4}$$

The spectral *tau* approach can be viewed as a special case of the Petrov-Galerkin that, applied to (2) reads:

$$\text{find } u_N \in W_N : \ a(u_N, v_N) = \mathcal{F}(v_N) \qquad \forall v_N \in V_N. \tag{5}$$

The *tau* method was proposed by Lanczos in 1938 ([16]), and it differs from the Galerkin one for the treatment of boundary conditions. In particular, the test functions are not required to satisfy the boundary conditions, since the latter are enforced through a set of supplementary equations. The projection operator $P_N$ is defined as for the Galerkin scheme. We refer to Sec. 1.2 for a more detailed description of tau approach.

Finally, the *collocation* approach is characterised by choosing $V_N = W_N$ as the space of lagrangian polynomials on a set of Gaussian quadrature nodes and by letting $P_N$ to be the interpolation operator with respect to the Gaussian quadrature formula.
The collocation form of (1) reads:

$$\text{find } u_N \in V_N : \ \begin{cases} L_N u_N = f & \text{at } \mathbf{x}_i \in \mathring{\Omega} \\ B_N u_N = 0 & \text{at } \mathbf{x}_i \in \partial\Omega, \end{cases} \tag{6}$$

where $L_N$ and $B_N$ are suitable approximations of $L$ and $B$, respectively, and $\mathbf{x}_i$ are the Gaussian nodes in $\overline{\Omega}$.

The use of a spectral scheme is also characterised by the way the solution $u_N \in W_N$ is represented, whether in *transform* or in *physical* space.
In transform space a function $v$ is described through its coefficients with respect to a complete orthogonal system (Fourier, Chebyshev or Legendre); in physical space by its nodal values in $\Omega$. For Galerkin or tau approaches, the solution is represented through the transform space, while for the collocation approach it will be represented in the physical space.

## 1.1 Fourier approximation

For a smooth and periodic complex function $u(x)$, defined on the interval $(0, 2\pi)$, its truncated Fourier series of order $N$ reads

$$P_N u(x) = \sum_{k=-N/2}^{N/2-1} \hat{u}_k \varphi_k(x), \tag{7}$$

with $\varphi_k(x) = e^{ikx}$.

For a suitable $N$, if $u \in \mathcal{C}^\infty(0, 2\pi)$ and it is periodic with all its derivatives in $(0, 2\pi)$, the truncated series (7) is a good approximation of $u$, thanks to the property that the $k-$th coefficient $\hat{u}_k$ of the expansion decays faster than any negative power of $k$. This property is usually referred to as "spectral accuracy" or "exponential accuracy" of the Fourier method.
More generally, given a periodic complex function $u$ defined on the domain $\Omega = (0, 2\pi)^d$ $(d = 2, 3)$, its truncated Fourier series will be:

$$P_N u(\mathbf{x}) = \sum_{k_1,..,k_d=-N/2}^{N/2-1} \hat{u}_{\mathbf{k}} \varphi_{\mathbf{k}}(\mathbf{x}), \tag{8}$$

where: $\mathbf{x} = (x_1, ..., x_d)$ will be an element of $\mathbb{R}^d$, $\mathbf{k} = (k_1, ..., k_d)$ a multi-index and $\varphi_{\mathbf{j}}(\mathbf{x}) = e^{i\mathbf{k}\cdot\mathbf{x}}$, with $\mathbf{k} \cdot \mathbf{x} = k_1 x_1 + ... + k_d x_d$.
The following result provides an estimate in all Sobolev norms for the remainder of the Fourier series of $u$:

$$\|u - P_N u\|_{H^s(\Omega)} \leq C N^{s-m} \|u\|_{H^m(\Omega)} \qquad \text{for } 0 \leq s \leq m. \tag{9}$$

Let us consider the differential problem

$$Lu = f \ \text{ in } \Omega = (0, 2\pi)^d, \qquad u \text{ periodic in } \Omega, \tag{10}$$

with $L$ being a differential operator and $f$ a suitable function defined in $\Omega = (0, 2\pi)^d$. We look for an approximate solution $u_N$ of $u$ by the Galerkin method (4) as follows. We define the space

$$V_N = span\{\varphi_{\mathbf{k}}(\mathbf{x}), \ -N/2 \leq k_j \leq N/2 - 1, \ j = 1, ..., d\} \tag{11}$$

and seek a function of the following form

$$u_N(\mathbf{x}) = \sum_{k_1,...,k_d=-N/2}^{N/2-1} \hat{a}_{\mathbf{k}} \varphi_{\mathbf{k}}(\mathbf{x}) \tag{12}$$

that satisfies the equations

$$\int_\Omega L u_N(\mathbf{x}) \overline{\varphi}_{\mathbf{k}}(\mathbf{x}) d\Omega = \int_\Omega f(\mathbf{x}) \overline{\varphi}_{\mathbf{k}}(\mathbf{x}) d\Omega \qquad -N/2 \leq k_1, .., k_d \leq N/2 - 1. \tag{13}$$

By the orthogonality of the Fourier system $\{\varphi_{\mathbf{k}}(\mathbf{x})\}$ in $V_N$, we obtain the following equations:

$$(\widehat{Lu_N})_{\mathbf{k}} = \hat{f}_{\mathbf{k}} \qquad -N/2 \le k_1, ..., k_d \le N/2 - 1, \tag{14}$$

where $\hat{f}_{\mathbf{k}}$ and $(\widehat{Lu_N})_{\mathbf{k}}$ are the coefficients of $f(\mathbf{x})$ and $Lu_N(\mathbf{x})$ respectively, with respect to the Fourier expansion.
We observe that 1-D differentiation of $P_N u$ in transform space consists of multiplying each Fourier coefficient $\hat{u}_k$ by the imaginary unity times the corresponding wavenumber, i.e.:

$$(P_N u)'(x) = P_N u'(x) = \sum_{k=-N/2}^{N/2-1} \hat{u}_k ik\varphi_k(x). \tag{15}$$

Similarly for partial derivatives we have:

$$\frac{\partial(P_N u)}{\partial x_j}(\mathbf{x}) = P_N \frac{\partial u}{\partial x_j}(\mathbf{x}) = \sum_{k_1,...,k_d=-N/2}^{N/2-1} \hat{u}_{\mathbf{k}} ik_j \varphi_{\mathbf{k}}(\mathbf{x}), \qquad j = 1, ..., d. \tag{16}$$

This implies that, if the operator $L$ is linear, the system (14) can be easily reduced to a diagonal system on the coefficients $\hat{a}_{\mathbf{k}}$ of (12). Otherwise convolution sums appear in the system which is not yet diagonal.

As an example of application of the Fourier-Galerkin method we consider the Helmholtz equation

$$\begin{cases} -\Delta u + \lambda u = f & \text{in } \Omega = (0, 2\pi)^2 \\ u \text{ periodic} & \text{in } \Omega \end{cases} \tag{17}$$

with $\lambda \ge 0$ and $f \in L^2(\Omega)$. The Fourier-Galerkin solution $u_N \in V_N$ satisfies the equation

$$\int_\Omega (-\Delta u_N(\mathbf{x}) + \lambda u_N(\mathbf{x})) e^{-i(k_1 x_1 + k_2 x_2)}\, d\Omega = \int_\Omega f(\mathbf{x}) e^{-i(k_1 x_1 + k_2 x_2)}\, d\Omega \qquad -N/2 \le k_1, k_2 \le N/2 - 1, \tag{18}$$

by (12), (16) and by the orthogonality of the basis in $V_N$ we obtain a diagonal system for the $(N+1)^2$ discrete Fourier coefficients $\{\hat{a}_{\mathbf{k}}\}$ :

$$(k_1^2 + k_2^2 + \lambda)\hat{a}_{\mathbf{k}} = \hat{f}_{\mathbf{k}} \qquad -N/2 \le k_1, k_2 \le N/2 - 1, \tag{19}$$

whose solution is very cheap. The coefficients $\hat{a}_{\mathbf{k}}$ are often named "frequency unknowns".
The Fourier Galerkin approach has pros and cons. Among the pros we note:

- its spectral accuracy (that we mentioned above), which means that, if $u \in H^s(\Omega)$, there exists a positive constant $C$ independent of $N$ such that (see [16])

  $$\|u - u_N\|_{H^m(\Omega)} \le C N^{m-s} \|u\|_{H^s(\Omega)} \qquad 0 \le m \le s,\ s \ge 0 \tag{20}$$

  (this makes spectral methods much more accurate than finite difference or finite element methods); ($H^r(\Omega)$ is the space of functions of $L^2(\Omega)$ whose distributional derivatives of order up to $r$ belong to $L^2(\Omega)$ (see [47]);

- the phase error is minimised; actually Fourier spectral methods are free of phase errors as $\varphi_k'(x) = ik\varphi_k(x),\ \forall k$;
- if $L$ is a linear differential operator with constant coefficients, then the system (14) is diagonal and only $\mathcal{O}(N)$ floating point operations are needed to compute the coefficients $\hat{a}_{\mathbf{k}}$.

On the other hand, the Fourier-Galerkin approach has several drawbacks:

- only periodic solutions can be treated;
- if the differential problem is non linear and/or it has non-constant coefficients, convolution sums appear in the system (14), with a consequently high computational effort.

The first drawback is overcome by using algebraic polynomials which preserve spectral accuracy (see Sec. 1.2), while for the latter, one resorts to the *pseudo-spectral Fourier method*, whose theoretical properties have been earlier pointed out in Gottlieb and Orszag ([36]) and in Kreiss and Oliger ([44]).

For simplicity of exposition we take now $d = 1$, a similar approach can be followed if $d > 1$ by building the set of nodes in $\Omega$ as a cartesian product of the one-dimensional sets of nodes.

We denote by

$$\Xi_N^G = \{x_j = \frac{2\pi}{N} j,\ j = 0, ..., N-1\} \tag{21}$$

the set of Gaussian nodes on the interval $[0, 2\pi]$, and by $I_N u \in V_N$ the trigonometric interpolant of $u$ on the set $\Xi_N^G$

$$I_N u(x) = \sum_{k=-N/2}^{N/2-1} \tilde{u}_k \varphi_k(x). \tag{22}$$

The coefficients

$$\tilde{u}_k = \frac{1}{N} \sum_{j=0}^{N-1} u(x_j) e^{-ikx_j} \qquad -N/2 \le k \le N/2 - 1 \tag{23}$$

are the "discrete Fourier coefficients" of the complex function $u$ in $[0, 2\pi]$ with respect to the nodes in $\Xi_N^G$. The polynomial (22) is also known as the discrete Fourier series of $u$ and (23) is the *discrete Fourier transform* from $N$ nodal values $\{u(x_j)\}$ to $N$ discrete coefficients $\{\tilde{u}_k\}$, (the latter being an approximation of $\{\hat{u}_k\}$). The interpolant (22) is preferred to the truncated series (7) since the coefficients $\hat{u}_k$ of an arbitrary function are not known in closed form, so that they must be approximated starting from the information in the physical space.

Due to the orthogonality of the Fourier system, we have the inversion formula or inverse discrete Fourier transform

$$u(x_j) = \sum_{k=-N/2}^{N/2-1} \tilde{u}_k e^{ikx_j} \qquad j = 0, ..., N-1. \tag{24}$$

The convergence properties of the interpolation polynomials $\{I_N u\}_{N\geq 0}$ are similar to those of the sequence of truncated Fourier series $\{P_N u\}_{N\geq 0}$, i.e.

$$\|u - I_N u\|_{H^s(\Omega)} \leq C N^{s-m} \|u\|_{H^m(\Omega)} \qquad \text{for } 0 \leq s \leq m,\ s \geq 0. \tag{25}$$

Furthermore, the continuous and the discrete Fourier coefficients ($\hat{u}_k$ and $\tilde{u}_k$) have the same asymptotic behaviour.

We define the *pseudo-spectral derivative* of $u(x)$ as the exact derivative of its interpolant polynomial $I_N u(x)$, i.e.

$$\mathcal{D}_N u := (I_N u)'. \tag{26}$$

If $u \notin V_N$ then $(I_N u)' \neq I_N(u')$, but the difference $\|(I_N u)' - I_N(u')\|$ is of the same order as $\|u' - P_N u'\|$ so that the pseudo spectral derivative is spectrally accurate. The Fourier pseudo-spectral derivative $\mathcal{D}_N u$ can be represented in the Gaussian nodes by a matrix-vector product, i.e.:

$$(\mathcal{D}_N u)(x_l) = \sum_{j=0}^{N-1} (D_N)_{lj} u(x_j) \qquad l = 0, ..., N-1 \tag{27}$$

with $D_N \in \mathbb{R}^{N\times N}$ and

$$(D_N)_{lj} = \begin{cases} \dfrac{1}{2}(-1)^{l+j} cot\left[\dfrac{(l-j)\pi}{N}\right] & l \neq j \\ 0 & l = j \end{cases} \qquad l, j = 0, ..., N-1. \tag{28}$$

The pseudo-spectral counterpart $L_N$ of a differential operator $L$ is obtained by substituting each derivative in $L$ by a pseudo-spectral derivative; for example, if $Lu := -(a\ u')' + (bu)' + cu$, with $a = a(x)$, $b = b(x)$ and $c = c(x)$, then the pseudo-spectral operator $L_N$ reads:

$$L_N u = -(I_N(a\ u'_N))' + (I_N(bu_N))' + cu_N. \tag{29}$$

In vector form (29) reads:

$$-D_N(\mathbf{a} \otimes (D_N \mathbf{u})) + D_N(\mathbf{b} \otimes \mathbf{u}) + \mathbf{c} \otimes \mathbf{u}, \tag{30}$$

where: $\mathbf{u} = (u_N(x_0), ..., u_N(x_{N-1}))^T$, $\mathbf{a} = (a(x_0), ..., a(x_{N-1}))^T$, $\mathbf{b} = (b(x_0), ..., b(x_{N-1}))^T$, $\mathbf{c} = (c(x_0), ..., c(x_{N-1}))^T$ and $\mathbf{a} \otimes \mathbf{b}$ denotes the point-wise product of two vectors $\mathbf{a}$ and $\mathbf{b}$.

We can now approximate the differential problem (1) at Gaussian nodes by a collocation approach by solving the system (not-diagonal in general):

$$L_N u_N(x_j) = f(x_j) \qquad \text{at } x_j \in \Xi_N^G. \tag{31}$$

The unknowns $\{u_N(x_j)\}_{j=0}^{N-1}$ of the system are said "physical unknowns", when they are available, an approximation $\tilde{a}_k$ of the frequency unknowns $\hat{a}_k$ (the coefficients of $u_N$ in (43)) can be computed via a discrete Fourier transform as follows:

$$\tilde{a}_k = \frac{1}{N} \sum_{j=0}^{N-1} u_N(x_j) e^{-ikx_j} \qquad -N/2 \leq k \leq N/2 - 1. \tag{32}$$

We observe that the discrete Fourier transform (23) can be used also to easily compute the pseudo-spectral derivative of a function $u$ that is known by its nodal values $u(x_j)$. In fact, in order to compute $\mathcal{D}_N u(x_j)$ one can "travel" from the nodal values $\{u(x_j),\ j = 0, ..., N-1\}$ to the discrete coefficients $\{\tilde{u}_k,\ -N/2 \leq k \leq N/2-1\}$ by a Discrete Fourier Transform (23), compute $\tilde{u}_k^{(1)} = ik\tilde{u}_k$ (which are the discrete coefficients of $\mathcal{D}_N u$) and then, go back to the physical space, by an inverse Discrete Fourier Transform (24).

A great impulse to the development of the pseudo-spectral Fourier approach was given by Cooley and Tukey ([23]) in 1965 by the introduction of the Fast Fourier Transform (FFT) algorithm that permits to compute the discrete Fourier coefficients $\{\tilde{u}_k\}$ from the nodal values $\{u_N(x_j)\}$ in $\mathcal{O}(N\ \log_2 N)$ floating point operations (provided that $N$ is a power of 2).

In order to treat the case of general boundary conditions, we introduce now the algebraic polynomial systems.

## 1.2 Galerkin spectral methods for problems with non-periodic boundary conditions

The property of spectral accuracy (20) is also attainable for smooth but non-periodic functions, provided that the expansion functions are properly chosen. Both Legendre and Chebyshev systems (see [16]) allow spectral accuracy in the expansion of smooth functions, they are algebraic polynomials and satisfy the orthogonality property with respect to a suitable weighted inner product in $L^2(-1,1)$.

From now on we denote by $\{T_k(x)\}_{k\geq 0}$ the set of Chebyshev polynomials:

$$\begin{array}{l} T_0(x) \equiv 1, \qquad T_1(x) = x, \\ T_{k+1}(x) = 2x\ T_k(x) - T_{k-1}(x) \quad k \geq 1 \end{array} \tag{33}$$

and by $\{L_k(x)\}_{k\geq 0}$ the set of Legendre polynomials:

$$\begin{array}{l} L_0(x) \equiv 1, \qquad L_1(x) = x, \\ L_{k+1}(x) = \dfrac{2k+1}{k+1} x L_k(x) - \dfrac{k}{k+1} L_{k-1}(x) \quad k \geq 1. \end{array} \tag{34}$$

They are orthogonal with respect to the weighted inner product

$$(u, v)_w := \int_{-1}^{1} u(x)v(x)w(x)dx, \tag{35}$$

where the weight is

$$w(x) = \begin{cases} \dfrac{1}{\sqrt{(1-x^2)}} & \text{for the Chebyshev system} \\ 1 & \text{for the Legendre system.} \end{cases} \tag{36}$$

The same notation used in (35) will be considered with functions defined on a two or three dimensional domain. In this case the weight will be the product of the weight functions given in (36) (see [16], Sec. 2.4 for more details).

### 1.2.1 The Galerkin approach

To deal with the weak formulation of (1) we denote by $H^1(\Omega)$ the space of functions $v \in L^2(\Omega)$ whose first-order distributional derivatives belong to $L^2(\Omega)$, endowed with the norm

$$\|v\|_{H^1(\Omega)} = \{\|v\|^2_{L^2(\Omega)} + \|\nabla v\|^2_{L^2(\Omega)}\}^{1/2}. \tag{37}$$

The symbol $H^1_0(\Omega)$ is used to denote the subspace of $H^1(\Omega)$ of the functions whose trace at the boundary is zero, i.e. $H^1_0(\Omega) = \{v \in H^1(\Omega) : \ v|_{\partial\Omega} = 0\}$.

Consider the Poisson equation in the unit square $\Omega = (-1,1)^2$ with homogeneous Dirichlet boundary condition:

$$-\Delta u = f \text{ in } \Omega, \qquad u = 0 \text{ on } \partial\Omega \tag{38}$$

and $f \in L^2(\Omega)$. This problem admits the variational form (2) with

$$V = H^1_0(\Omega), \quad a(u,v) = \int_\Omega \nabla u \cdot \nabla v d\Omega \ \text{ and } \ \mathcal{F}(v) = \int_\Omega fv \ d\Omega. \tag{39}$$

We denote by $\mathbb{P}_N(I)$ the set of the algebraic polynomials of degree less than or equal to $N$ on the interval $I \subset \mathbb{R}$, and by $\mathbb{Q}_N(\Omega)$ the set of algebraic polynomials of degree less than or equal to $N$ in each variable in $\Omega$. Then we look for the solution of the Galerkin method taking

$$V_N = \{v \in \mathbb{Q}_N(\Omega) : v = 0 \text{ on } \partial\Omega\} \tag{40}$$

We choose in $V_N$ the following basis functions $\varphi_{\mathbf{k}}(\mathbf{x}) = \varphi_{k_1}(x_1)\varphi_{k_2}(x_2)$, $2 \le k_1, k_2 \le N$ with

$$\varphi_k(x) = \begin{cases} T_k(x) - T_0(x) & k \text{ even} \\ T_k(x) - T_1(x) & k \text{ odd} \end{cases} \tag{41}$$

or

$$\varphi_k(x) = \begin{cases} L_k(x) - L_0(x) & k \text{ even} \\ L_k(x) - L_1(x) & k \text{ odd.} \end{cases} \tag{42}$$

Then we expand the numerical solution $u_N$ with respect to this basis:

$$u_N(\mathbf{x}) = \sum_{k_1,k_2=2}^{N} a_{\mathbf{k}}\varphi_{\mathbf{k}}(\mathbf{x}). \tag{43}$$

Since the basis functions $\varphi_{\mathbf{k}}(\mathbf{x})$ satisfy the homogeneous Dirichlet boundary conditions given in (38) no explicit boundary conditions will be imposed on $u_N$.

The Galerkin formulation of (38) reads:

$$\text{find } \ u_N \in V_N : \qquad (\nabla u_N, \nabla\varphi_{\mathbf{j}})_w = (f, \varphi_{\mathbf{j}})_w \qquad 2 \le j_1, j_2 \le N \tag{44}$$

and owing to (43), this yields the following system for the $\{a_{\mathbf{k}}\}$ :

$$\sum_{k_1,k_2=2}^{N} a_{\mathbf{k}}(\nabla\varphi_{\mathbf{k}}, \nabla\varphi_{\mathbf{j}})_w = (f, \varphi_{\mathbf{j}})_w \qquad 2 \le j_1, j_2 \le N. \tag{45}$$

The matrix form of (45) reads:

$$S\mathbf{a} = \mathbf{f} \tag{46}$$

where $S = [(\nabla\varphi_{\mathbf{k}}, \nabla\varphi_{\mathbf{j}})_w]$ is the stiffness matrix, $\mathbf{a} = [a_{\mathbf{k}}]$ is the vector of unknowns and $\mathbf{f} = [(f, \varphi_{\mathbf{j}})_w]$ is the right hand side.
The matrix $S$ is a structured sparse matrix and it is symmetric only if the Legendre system is used.
We observe that, in general, this approach is scarcely used in the spectral context since, for large values of $N$, a large computational effort is required to evaluate both the bilinear form and the right hand side by sufficiently accurate quadrature formulas.

### 1.2.2 The spectral tau approach

The main feature of this approach is that the test space $V_{_N}$ and the trial space $W_{_N}$ do not coincide. As for the Galerkin approach the operator $P_{_N}$ is the orthogonal projection operator from $W$ to $V_{_N}$ relative to the inner product of $V$. Let $\Xi_N^{CGL}$ be the set of nodes of the Gauss-Lobatto quadrature formulas of Chebyshev type:

$$\Xi_N^{CGL} = \{\xi_0 = -1,\ \xi_i = -cos(i\pi/N),\ i = 1, ..., N-1,\ \ \xi_N = 1\} \tag{47}$$

and $\Xi_N^{LGL}$ the set of Legendre type:

$$\Xi_N^{LGL} = \{\xi_0 = -1,\ \ \xi_N = 1,\ \xi_i, i = 1, ..., N-1,\ \text{are the zeros of } L'_N(\xi)\}. \tag{48}$$

Then we define $\mathbf{\Xi}_N^{CGL} = \Xi_N^{CGL} \times \Xi_N^{CGL}$ and denote by $\mathbf{x}_{ij} = (\xi_i, \xi_j)$ its elements. (The same notation holds for the Legendre set of nodes). We consider the problem (1) on the computational domain $\Omega \subset \mathbb{R}^2$ and the Petrov-Galerkin approach (5), where we define the trial space as

$$W_{_N} = \{v \in \mathbb{Q}_{_N}(\Omega) :\ Bv(\mathbf{x}_{ij}) = 0 \text{ at } \mathbf{x}_{ij} \in \partial\Omega\}, \tag{49}$$

while the choice of $V_{_N}$ depends on the number of boundary conditions which are imposed on each side of $\partial\Omega$.

As an example we consider the Neumann problem for a second-order elliptic operator in the interval $(-1, 1)$:

$$\begin{cases} Lu := -u'' + u = f & -1 < x < 1 \\ u'(-1) = u'(1) = 0, \end{cases} \tag{50}$$

and we look for the tau solution

$$u_{_N} \in W_{_N} = \{v \in \mathbb{P}_{_N}(-1, 1) :\ v'(-1) = v'(1) = 0\} \tag{51}$$

expanded in Chebyshev polynomials, i.e.: $u_{_N}(x) = \sum_{k=0}^{N} \tilde{a}_k T_k(x)$.

Here $V_{_N} = \mathbb{P}_{_{N-2}}(-1,1) = span\{T_k(x),\ k = 0, ..., N-2\}$ and the solution $u_{_N}$ is determined by the system:

$$\begin{cases} \int_{-1}^{1} (-u''_{_N} + u_{_N})(x) T_k(x) w(x)\ dx = \int_{-1}^{1} f(x) T_k(x) w(x)\ dx \\ \qquad\qquad\qquad\qquad\qquad\qquad \text{for } k = 0, .., N-2 \\ u'_{_N}(-1) = u'_{_N}(1) = 0. \end{cases} \tag{52}$$

Since the derivatives of $u_{_N}$ can be expanded with respect to the Chebyshev system as follows (see [16], Sec. 2.4.2):

$$u'_{_N}(x) = \sum_{k=0}^{N-1} \tilde{a}_k^{(1)} T_k(x) \tag{53}$$

with

$$\tilde{a}_k^{(1)} = \frac{2}{c_k} \sum_{\substack{p=k+1 \\ p+k\ odd}}^{N} p \tilde{a}_p \qquad c_0 = 2,\ c_k = 1 \text{ for } k \geq 1, \tag{54}$$

and

$$u''_{_N}(x) = \sum_{k=0}^{N-2} \tilde{a}_k^{(2)} T_k(x) \tag{55}$$

with

$$\tilde{a}_k^{(2)} = \frac{1}{c_k} \sum_{\substack{p=k+2 \\ p+k\ even}}^{N} p(p^2 - k^2) \tilde{a}_p, \tag{56}$$

we can transform the system (52) in terms of the unknown coefficients $\{\tilde{a}_k\}$ and obtain:

$$\begin{cases} -\frac{1}{c_k} \sum_{\substack{p=k+2 \\ p+k\ even}}^{N} p(p^2 - k^2) \tilde{a}_p + \tilde{a}_k = \hat{f}_k \qquad\qquad k = 0, ..., N-2 \\ \sum_{k=0}^{N-1} \frac{(-1)^k}{c_k} \sum_{\substack{p=k+1 \\ p+k\ odd}}^{N} p \tilde{a}_p = \sum_{k=0}^{N-1} \frac{1}{c_k} \sum_{\substack{p=k+1 \\ p+k\ odd}}^{N} p \tilde{a}_p = 0. \end{cases} \tag{57}$$

Following [16] (Sec. 5.1.2), the Neumann boundary conditions in (57) can be rewritten as

$$\sum_{\substack{k=1 \\ k\ odd}}^{N} k^2 \tilde{a}_k = \sum_{\substack{k=2 \\ k\ even}}^{N} k^2 \tilde{a}_k = 0, \tag{58}$$

so that the even and odd coefficients in (57) can be decoupled and a block diagonal linear system has to be solved.
The matrix associated to the linear system for the even (or odd) coefficients has an upper Hessenberg structure and a Gauss elimination without pivoting can be used with a computational effort of the order of $N^2/4$ operations.

In general the accuracy of this approach is less than the one from Galerkin's approach if the same number of degrees of freedom is used.

We have seen that both Galerkin and tau spectral methods are formulated in terms of the frequency unknowns $\{\tilde{a}_k\}$ of the numerical solution $u_N$. As such, they are cumbersome to handle for general problems with variables coefficients and/or nonlinearities, due to the presence of convolution sums. As already seen in the periodic case, this leads to the use of spectral methods with nodal variables, i.e. to collocation or generalized Galerkin spectral methods.

### 1.3 Collocation spectral methods

These collocation methods are in general amenable to Galerkin spectral methods since they make use of Gaussian nodes for the numerical evaluation of integrals.
Consider the two-dimensional elliptic problem with homogeneous Dirichlet boundary conditions:

$$\begin{cases} Lu := -\nabla \cdot (\nu \nabla u) + \gamma u = f & \text{in } \Omega = (-1,1)^2 \\ u = 0 & \text{on } \partial\Omega \end{cases} \tag{59}$$

with $f \in L^2(\Omega)$, $\nu,\ \gamma \in L^\infty(\Omega)$ non negative.
Given $N \geq 2$, we consider the 2-D Chebyshev Gauss-Lobatto set $\boldsymbol{\Xi}_N^{CGL}$ (or the Legendre Gauss-Lobatto set $\boldsymbol{\Xi}_N^{LGL}$) and we look for a function $u_N \in \mathbb{Q}_N(\Omega)$ such that:

$$\begin{cases} -\nabla \cdot (\nu(\mathbf{x}_{ij}) \nabla u_N(\mathbf{x}_{ij})) + \gamma(\mathbf{x}_{ij}) u_N(\mathbf{x}_{ij}) = f(\mathbf{x}_{ij}) & \forall \mathbf{x}_{ij} \in \mathring{\Omega} \\ u_N(\mathbf{x}_{ij}) = 0 & \forall \mathbf{x}_{ij} \in \partial\Omega. \end{cases} \tag{60}$$

The system (60) is referred to as the *point-wise form of the spectral collocation method.*

The primary unknowns of the collocation problem (60) are the nodal values $u_N(\mathbf{x}_{ij})$. They are computed by solving the linear system that arises from the pseudo-spectral approximation of (60), i.e. by substituting each derivative in (59) by a pseudo spectral derivative as done for the Fourier expansion.

In order to derive the algebraic form of (60) we introduce the Lagrangian basis functions associated to the nodes $\Xi_N^{CGL}$ or $\Xi_N^{LGL}$:

$$\psi_i \in \mathbb{P}_N(-1,1),\ \psi_i(\xi_j) = \delta_{ij},\ i,j = 0,...,N, \tag{61}$$

and the 2-D Lagrangian basis associated to the sets $\boldsymbol{\Xi}_N^{CGL}$ or $\boldsymbol{\Xi}_N^{LGL}$ defined by a tensorial product as:

$$\varphi_{ij}(\mathbf{x}) = \psi_i(x_1)\psi_j(x_2) \in \mathbb{Q}_N(\Omega),\ i,j = 0,...,N. \tag{62}$$

Clearly $\varphi_{ij}(\mathbf{x}_{kl}) = \delta_{ik}\delta jl$. The Lagrange interpolant of $u \in \mathcal{C}^0(\overline{\Omega})$ on the nodes of $\Xi_N^{LGL}$ or $\Xi_N^{CGL}$ is

$$I_{_N} u(\mathbf{x}) = \sum_{i,j=0}^{N} u(\mathbf{x}_{ij})\varphi_{ij}(\mathbf{x}), \tag{63}$$

and the solution $u_{_N}(\mathbf{x})$ of (60) reads:

$$u_{_N}(\mathbf{x}) = \sum_{i,j=0}^{N} u_{_N}(\mathbf{x}_{ij})\varphi_{ij}(\mathbf{x}). \tag{64}$$

The pseudo-spectral partial derivatives of a regular function $u$ are defined as follows:

$$(\mathcal{D}_{_{N,x_m}} u)(\mathbf{x}) = \frac{\partial I_{_N} u}{\partial x_m}(\mathbf{x}) = \sum_{i,j=0}^{N} u(\mathbf{x}_{ij}) \frac{\partial \varphi_{ij}}{\partial x_m}(\mathbf{x}), \quad m = 1, 2. \tag{65}$$

Setting

$$(D_{_{N,1}})_{kl,ij} = \frac{\partial \varphi_{ij}}{\partial x_1}(\mathbf{x}_{kl}), \qquad\qquad (D_{_{N,2}})_{kl,ij} = \frac{\partial \varphi_{ij}}{\partial x_2}(\mathbf{x}_{kl}), \tag{66}$$

for $i, j, k, l = 0, ..., N$, they can be represented by the matrix-vector form:

$$(\mathcal{D}_{_{N,x_m}})u(\mathbf{x}_{kl}) = \sum_{i,j=0}^{N} (D_{N,m})_{kl,ij}\ u(\mathbf{x}_{ij}), \qquad m = 1, 2. \tag{67}$$

The squared matrices in (66) of order $(N+1)^2$, are the "pseudo-spectral derivative matrices". They have a sparse structure, with $(N+1)^3$ non-zero entries.
As for the Fourier system, an alternative way to compute the pseudo-spectral derivative of $u$ consists in passing from the physical space to the frequency space, differentiating and then coming back to the physical space. This procedure is efficient for Chebyshev expansions for large $N$, as a fast transform is still available.

When $\Omega$ is a rectangular domain, the matrices (66) can be obtained from their one-dimensional counterpart, the pseudo-spectral derivative matrix $D_N$, of order $(N+1)$. In fact, the $x_1$ (resp. $x_2$) pseudo-spectral derivative is the same on all rows (resp. columns) of the collocation grid, i.e.

$$(\mathcal{D}_{_{N,x_1}})(\mathbf{x}_{kl}) = \psi_i'((x_1)_k)\psi_j((x_2)_l) = \psi_i'((x_1)_k)\delta_{jl} \tag{68}$$

and

$$(\mathcal{D}_{_{N,x_2}})(\mathbf{x}_{kl}) = \psi_i((x_1)_k)\psi_j'((x_2)_l) = \delta_{ik}\psi_j'((x_2)_l). \tag{69}$$

If we consider the set of Chebyshev Gauss-Lobatto nodes (47), and we write the Lagrange polynomials $\psi_i(x_1)$, $\psi_j(x_2)$ in terms of the Chebyshev functions, the

pseudo-spectral derivative matrix in one dimension has the following entries:

$$(D_N)_{lj} = \begin{cases} \dfrac{\overline{c}_l}{\overline{c}_j}\dfrac{(-1)^{l+j}}{\xi_l - \xi_j} & l \neq j \\ \dfrac{-\xi_j}{2(1-\xi_j^2)} & 1 \leq l = j \leq N-1 \\ -\dfrac{2N^2+1}{6} & l = j = 0 \\ \dfrac{2N^2+1}{6} & l = j = N \end{cases} \tag{70}$$

with

$$\overline{c}_l = \begin{cases} 2 & l = 0, N \\ 1 & 1 \leq l \leq N-1. \end{cases} \tag{71}$$

Similarly, for the Legendre system (48) we have:

$$(D_N)_{lj} = \begin{cases} \dfrac{L_N(x_l)}{L_N(x_l)}\dfrac{1}{\xi_l - \xi_j} & l \neq j \\ 0 & 1 \leq l = j \leq N-1 \\ -\dfrac{(N+1)N}{4} & l = j = 0 \\ \dfrac{(N+1)N}{4} & l = j = N. \end{cases} \tag{72}$$

The system (60) can be written in matrix form through the following matrix

$$A^c_{sp} = -D_{N,1} V D_{N,1} - D_{N,2} V D_{N,2} + G \tag{73}$$

with $V_{ij,kl} = \nu(\mathbf{x}_{ij})\delta_{ik}\delta_{jl}$ and $G_{ij,kl} = \gamma(\mathbf{x}_{ij})\delta_{ik}\delta_{jl}$ (for $i,j,k,l, = 0, ..., N$).
The matrix $A^c_{sp}$ is the algebraic counterpart of the differential operator of (60). Its structure is represented in Fig. 1. By substituting the rows of $A^c_{sp}$ associated to the boundary nodes with the rows of the identity matrix (corresponding to Dirichlet boundary conditions), the algebraic form of (60) reads

$$A^c_{sp}\mathbf{u} = \mathbf{f} \tag{74}$$

where

$$\mathbf{u}_{ij} = u_N(\mathbf{x}_{ij}), \text{ and } \mathbf{f}_{ij} = \begin{cases} f(\mathbf{x}_{ij}) & \forall \mathbf{x}_{ij} \in \mathring{\Omega} \\ 0 & \forall \mathbf{x}_{ij} \in \partial\Omega. \end{cases} \tag{75}$$

We observe that the system can be reduced by eliminating the unknowns associated to the nodes on the boundary.
The condition number of $A^c_{sp}$ is $\chi_{sp}(A^c_{sp}) = \mathcal{O}(N^4)$ so that, when using iterative methods, the use of preconditioners is mandatory.

In 1980 Orszag introduced the centred finite difference preconditioner, i.e. the matrix obtained by the approximation of the same differential operator by finite

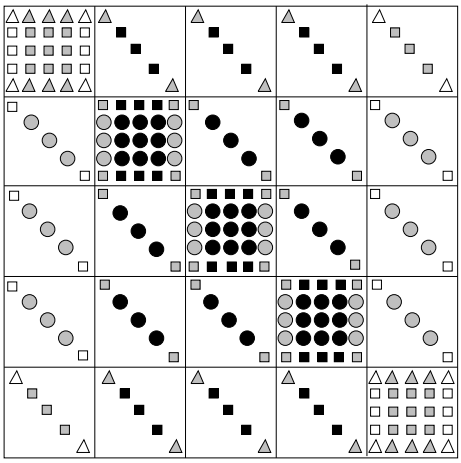

Figure 1: The pattern of matrix $S$

difference on the Gauss-Lobatto grid. This is an optimal preconditioner for the spectral collocation since the eigenvalues of the centred finite difference derivative matrix on the Gauss-Lobatto grid and the pseudo-spectral matrix $D_N$ have the same asymptotic behaviour.
Later, in 1985, the finite element matrix was proposed by Deville and Mund ([25]) and by Canuto and Quarteroni ([20]), using bilinear finite elements on the grid induced by the Gauss-Lobatto nodes. Effective generalizations of the finite element preconditioner have been carried out later by Canuto and Pietra ([18]), Deville and Mund ([26]) and by Quarteroni and Zampieri ([73]). For elliptic equations, both finite differences and finite elements matrices lead to a preconditioned matrix whose condition number is independent of $N$, see Haldenwang, Labrosse, Abboudi and Deville ([38]).

### 1.4 Generalized Galerkin method

The Generalized Galerkin (GG) method is obtained from a Galerkin method in which every integral is replaced by suitable quadrature formulas.
In particular for the spectral methods, the Gauss-Lobatto quadrature formulas are used. For any function $u \in \mathcal{C}^0([-1,1])$ the Gauss Lobatto quadrature formulas read as follows:

$$\int_{-1}^{1} u(\xi) w(\xi) d\xi \simeq \sum_{i=0}^{N} u(\xi_i) w_i, \tag{76}$$

where the values $\xi_i$ and $w_i$ are said respectively nodes and weights of the quadrature formulas. The nodes of the Chebyshev Gauss-Lobatto quadrature formulas are those given in (47) and the weights are

$$w_i = \begin{cases} \dfrac{\pi}{2N} & i = 0, N \\ \dfrac{\pi}{N} & i = 1, ..., N-1, \end{cases} \tag{77}$$

while the Legendre Gauss-Lobatto nodes are those given in (48) and the weights are:

$$w_i = \frac{2}{N(N+1)} \frac{1}{L_N^2(\xi_j)} \qquad i = 0, ..., N. \tag{78}$$

The Gauss-Lobatto quadrature formulas are exact for polynomials of degree less than or equal to $2N-1$. For any fixed $N \geq 1$, the nodes for 2-D quadrature formulas are those given in $\Xi_N^{LGL}$ or $\Xi_N^{CGL}$ and the weights are $w_{ij} = w_i w_j$ for $i, j = 0, ..., N$. Then, $\forall u, v \in \mathcal{C}^0(\overline{\Omega})$, we define the discrete scalar product:

$$(u, v)_{N,\Omega} = \sum_{i,j=0}^{N} u(\mathbf{x}_{ij}) v(\mathbf{x}_{ij}) w_{ij} \tag{79}$$

and we note that

$$(u, 1)_{N,\Omega} = \int_{\Omega} u(\mathbf{x}) w(\mathbf{x}) \mathrm{d}\Omega \qquad \forall u \in \mathbb{Q}_{2N-1}(\Omega). \tag{80}$$

The interpolation on the Legendre Gauss-Lobatto nodes satisfies the following bounds (see [19]): if $u \in H^s(\Omega)$, for some $s \geq 2$

$$\|u - I_N u\|_{H^k(\Omega)} \leq C N^{k-s} \|u\|_{H^s(\Omega)} \qquad \text{for } k = 0, 1. \tag{81}$$

Thanks to (81) it holds that: if $u \in H^s(\Omega)$, for some $s \geq 2$ and $v_N \in \mathbb{Q}_N(\Omega)$, then there exists $C > 0$ independent of $N$ such that

$$|(u, v_N)_{L^2(\Omega)} - (u, v_N)_{N,\Omega}| \leq C N^{-s} \|u\|_{H^s(\Omega)} \|v_N\|_{L^2(\Omega)}. \tag{82}$$

Similar estimates hold for the interpolation on the Chebyshev Gauss-Lobatto nodes, by replacing the classical Sobolev norm in $H^k$ with the weighted Sobolev norm.

By setting $V_N = \mathbb{Q}_N(\Omega) \cap H_0^1(\Omega)$, and

$$a_N(u_N, v_N) := (\nu \nabla u_N, \nabla v_N)_{N,\Omega} + (\gamma u_N, v_N)_{N,\Omega} \qquad \forall u_N, v_N \in V_N, \tag{83}$$

the GG formulation of problem (59) reads:

$$\text{find } u_N \in V_N : \qquad a_N(u_N, v_N) = (f, v_N)_{N,\Omega} \qquad \forall v_N \in V_N. \tag{84}$$

In the case of Dirichlet boundary condition, the Generalized Galerkin approach is equivalent to the collocation approach introduced in the previous section.
For all $u_N, v_N \in \mathbb{Q}_N(\Omega)$ we start noticing that

$$(\nu \nabla u_N, \nabla v_N)_{N,\Omega} = -(\nabla \cdot I_N(\nu \nabla u_N), v_N)_{N,\Omega} + \sum_{k=1}^{4} \left( \nu \frac{\partial u_N}{\partial \mathbf{n}}, v_N \right)_{N,S_k} \tag{85}$$

where $S_k$ denotes the $k-$th side of the boundary $\partial\Omega$ and $\mathbf{n}$ the outward normal vector to $\partial\Omega$. To obtain the system (60) starting from (84), it is sufficient to put $v_N(\mathbf{x}) = \varphi_{ij}$ (for $i, j = 1, ..., N-1$) in (84), use the identity (85) and to eliminate the sum in (85) thanks to the homogeneous Dirichlet boundary conditions.

By the linearity of the problem and by (43), the generalized Galerkin formulation (84) also reads:

$$\sum_{k,l=0}^{N} a_{_N}(\varphi_{kl},\varphi_{ij})u_{_N}(\mathbf{x}_{kl}) = (f,\varphi_{ij})_{_{N,\Omega}} \qquad i,j = 0,...,N, \tag{86}$$

or again

$$A_{sp}\mathbf{u} = \mathbf{f} \tag{87}$$

with $(A_{sp})_{ij,kl} = a_{_N}(\varphi_{kl},\varphi_{ij})$ and $(\mathbf{f})_{ij} = (f,\varphi_{ij})_{_{N,\Omega}}$ for the internal nodes, $(A_{sp})_{ij,kl} = \delta_{ki}\delta_{lj}$ and $(\mathbf{f})_{ij} = 0$ for the Dirichlet boundary nodes.

The matrix $A_{sp}$ differs from the collocation matrix $A^c_{sp}$ on the rows associated to internal nodes, for the presence of the quadrature weights, more precisely:

$$(A_{sp})_{ij,kl} = w_{ij}(A^c_{sp})_{ij,kl} \qquad \forall i,j,k,l = 1,...,N-1. \tag{88}$$

Even if the collocation and the GG approaches are equivalent, the latter formulation is often preferred, in fact:

1. the condition number of $A_{sp}$ is $\chi(A_{sp}) = \mathcal{O}(N^3)$ versus $\chi(A^c_{sp}) = \mathcal{O}(N^4)$;
2. by eliminating the rows and the columns associated to the Dirichlet nodes, the matrix $A_{sp}$ becomes symmetric.

Collocation and GG approaches differ on the treatment of Neumann data. Set $\mathbf{n} = (n_x, n_y)$ and assign the Neumann boundary condition $\partial u/\partial\mathbf{n} = g$ on an open subset $\partial\Omega_{_N}$ of $\partial\Omega$, with $g \in L^2(\partial\Omega_{_N})$.
When using a collocation approach, the Neumann boundary condition is strongly enforced on the boundary nodes and it reads:

$$\begin{aligned}\nu(\mathbf{x}_{ij})\frac{\partial u_{_N}}{\partial\mathbf{n}}(\mathbf{x}_{ij}) &= \nu(\mathbf{x}_{ij})\frac{\partial u_{_N}}{\partial x}(\mathbf{x}_{ij})n_x(\mathbf{x}_{ij}) + \nu(\mathbf{x}_{ij})\frac{\partial u_{_N}}{\partial y}(\mathbf{x}_{ij})n_y(\mathbf{x}_{ij}) \\ &= \nu(\mathbf{x}_{ij})n_x(\mathbf{x}_{ij})(D_{N,1}\mathbf{u})_{ij} + \nu(\mathbf{x}_{ij})n_y(\mathbf{x}_{ij})(D_{N,2}\mathbf{u})_{ij} = g(\mathbf{x}_{ij}).\end{aligned} \tag{89}$$

The matrix $A^c_{sp}$ is updated on the rows associated to Neumann boundary nodes with the terms $(A^c_{sp})_{ij,kl} = \nu(\mathbf{x}_{ij})n_x(\mathbf{x}_{ij})(D_{N,1})_{ij,kl} + \nu(\mathbf{x}_{ij})n_y(\mathbf{x}_{ij})(D_{N,2})_{ij,kl}$.

Otherwise, thanks to the equivalence (85), inside the GG approach the Neumann condition is expressed in weak form by the equations

$$a_{_N}(u_{_N},\varphi_{ij}) = (f,\varphi_{ij})_{_{N,\Omega}} + \sum_{\substack{k=1\\ S_k\subset\partial\Omega_{_N}}}^{4} (g,\varphi_{ij|S_k})_{_{N,S_k}}, \qquad \forall i,j:\ \mathbf{x}_{ij}\in\partial\Omega. \tag{90}$$

The matrix $A_{sp}$ is not changed, while now the component $\mathbf{f}_{ij}$ of the right hand side will contain the right hand side of (90). It is worthwhile observing that Neumann boundary conditions expressed in weak form do not affect the symmetry of the matrix $A_{sp}$, contrary to what happens for the strong form (89).

For the convergence analysis, the Strang lemma ([71]) can be advocated. For that consider the linear differential problem (1) and the following GG approximation:

$$\text{find } u_{_N}\in V_{_N} : a_{_N}(u_{_N},v_{_N}) = \mathcal{F}_{_N}(v_{_N}) \qquad \forall v_{_N}\in V_{_N}. \tag{91}$$

**Theorem 1.1 (Strang lemma)** Let $V$ be a Hilbert space endowed with the norm $\|\cdot\|$, $a : V \times V \to \mathbb{R}$ a bilinear and continuous form, i.e.:

$$\exists \gamma > 0 : \ |a(w,v)| \leq \gamma \|w\| \ \|v\| \qquad \forall w, v \in V \tag{92}$$

and $\mathcal{F} : V \to \mathbb{R}$ a linear continuous functional.
Suppose further that $\mathcal{F}_N(\cdot)$ is a linear map and the bilinear form $a_N(\cdot,\cdot)$ is uniformly coercive over $V_N \times V_N$. This means that there exists a positive constant $\alpha^*$ such that for all $N \geq 1$ it holds

$$a_N(v_N, v_N) \geq \alpha^* \|v_N\|^2 \qquad \forall v_N \in V_N. \tag{93}$$

Then there exists a unique solution $u_N$ of (91), which satisfies

$$\|u_N\| \leq \frac{1}{\alpha^*} \sup_{\substack{v_N \in V_N \\ v_N \neq 0}} \frac{\mathcal{F}_N(v_N)}{\|v_N\|}. \tag{94}$$

Moreover, if $u$ is the solution to (2), then

$$\begin{aligned} \|u - u_N\| \leq \ & \inf_{w_N \in V_N} \Big[ \Big(1 + \frac{\gamma}{\alpha^*}\Big) \|u - w_N\| \\ & + \frac{1}{\alpha^*} \sup_{\substack{v_N \in V_N \\ v_N \neq 0}} \frac{|a(w_N, v_N) - a_N(w_N, v_N)|}{\|v_N\|} \Big] \\ & + \frac{1}{\alpha^*} \sup_{\substack{v_N \in V_N \\ v_N \neq 0}} \frac{|\mathcal{F}(v_N) - \mathcal{F}_N(v_N)|}{\|v_N\|}. \square \end{aligned} \tag{95}$$

If we take $V = H_0^1(\Omega)$, if the bilinear form $a_N$ is that given in (83), $\mathcal{F}_N(v_N) := (f, v_N)_{N,\Omega}$ and $u_N$ is the GG solution of (84), we have a more detailed result. In fact, by taking the interpolant of $u$ of degree $N-1$ in each variable in place of $w_N$ in (95), the term $\|u - w_N\|_{H^1(\Omega)}$ is bounded by $C(N-1)^{1-s}\|u\|_{H^s(\Omega)}$ (by the inequality (81)) and the difference $|a(w_N, v_N) - a_N(w_N, v_N)|$ is equal to zero. Finally, for some $r > 1$, the term $|\mathcal{F}(v_N) - \mathcal{F}_N(v_N)|$ is bounded by $CN^{-r}\|f\|_{H^r(\Omega)}\|v_N\|_{L^2(\Omega)}$ (by (82)), so that

$$\|u - u_N\|_{H^1(\Omega)} \leq C(N^{1-s}\|u\|_{H^s(\Omega)} + N^{-r}\|f\|_{H^r(\Omega)}). \tag{96}$$

## 1.5 The spectral element method

Spectral Element Method (SEM) combines the high accuracy of spectral approximation to (at some extent) the geometric versatility of the Finite Element Method. The computational domain is partitioned into macro "spectral" elements, either quadrilateral or triangular then, a Generalized Galerkin formulation based on Gaussian quadrature formulas and relatively high degree polynomials are used.
SEM are very similar to some $h-p$ type Finite Element (see [3]), the essential difference between the two approaches lies in the choice of the basis for the trial and the test functions of the variational formulation.

SEM were proposed by Patera in 1984 ([62]); initially, conforming partitions in rectangular domains were considered. Later, Korczak and Patera ([43]) adopted

the isoparametric mappings (largely used in FEM) in order to discretize more complex geometries. In 1989 Bernardi, Maday and Patera ([6]) introduced a new non-conforming approach to domain decomposition: the mortar element method, and Mavripilis, Maday and Patera ([49]) applied it to the spectral approximation. The latter has become very competitive in the treatment of complex geometries with non-uniform distribution of the computational nodes (see [6], [49]).
In 1991 Dubiner ([29]) and later Karnadiakis ([78]) gave a great impulse to triangular spectral elements, by the use of orthogonal polynomial basis on triangular domains.

Now we confine to continuous and conforming spectral elements for ease of exposition. In order to briefly illustrate the conforming SEM we introduce in $\Omega$ a decomposition $\mathcal{T}_H$ of quadrilaterals $T_k$, with $k = 1, ..., Ne$, we set

$$H = \max_{T_k \in \mathcal{T}_H} \text{diam}(T_k) \qquad \text{diam}(T_k) = \max \text{diag}(T_k) \tag{97}$$

and we use the set $\Xi_N^{LGL}$ of Legendre Gauss-Lobatto nodes (48) on each element $T_k$. Then we set:

$$V_{\mathcal{H}} = \{u_{\mathcal{H}} \in \mathcal{C}^0(\overline{\Omega}) : \ u_{\mathcal{H}}|_{T_k} \in \mathbb{Q}_{N}(T_k), \ \forall T_k \in \mathcal{T}_H\} \tag{98}$$

and $u_{N,k} = u_{\mathcal{H}}|_{T_k}$, $v_{N,k} = v_{\mathcal{H}}|_{T_k}$. The discretization of (2) by the SEM reads:

$$\text{find } u_{\mathcal{H}} \in V_{\mathcal{H}} : \qquad \sum_{k=1}^{Ne} a_{N,k}(u_{N,k}, v_{N,k}) = \sum_{k=1}^{Ne} (f, v_{N,k})_{N,k} \qquad \forall v_{\mathcal{H}} \in V_{\mathcal{H}} \tag{99}$$

where $a_{N,k}(u_{N,k}, v_{N,k})$ is obtained from $a|_{T_k}(u_{\mathcal{H}}, v_{\mathcal{H}})$ by replacing each integral with the Legendre Gauss-Lobatto quadrature formulas, and $(f, v_{N,k})_{N,k}$ is the Legendre Gauss-Lobatto numerical integration of $\int_{T_k} f v_{N,k} \, \mathrm{d}T_k$.

The following interpolation and quadrature error formulas hold (see [34]):

**Theorem 1.2** For all $u \in H^s(\Omega)$ with $s \geq 2$, there exists a constant $C_1 > 0$ independent of $H_k$ and $N$ such that $\forall T_k \in \mathcal{T}_H$

$$\|u - I_N u\|_{H^m(T_k)} \leq C_1 H_k^{\min(N+1,s)-m} N^{m-s} \|u\|_{H^s(T_k)} \qquad m = 0, 1. \tag{100}$$

Moreover, there exists a constant $C_2 > 0$ independent of $H$ and $N$ such that

$$\|u - I_{\mathcal{H}} u\|_{H^m(\Omega)} \leq C_2 H^{\min(N+1,s)-m} N^{m-s} \|u\|_{H^s(\Omega)} \qquad m = 0, 1. \square \tag{101}$$

**Lemma 1.3** If $u \in H^s(T_k)$ with $s \geq 2$, then $\exists C > 0$ independent of $N$ and $H$ such that $\forall v_N \in \mathbb{Q}_N(T_k)$

$$|(u, v_N)_{L^2(T_k)} - (u, v_N)_{N,T_k}| \leq C(s) N^{-s} H^{\min(N+1,s)} \|u\|_{H^s(T_k)} \|v_N\|_{L^2(T_k)}. \square \tag{102}$$

On the basis of these results, if $u$ is the solution to (59), $u_{\mathcal{H}}$ to (99) and $f \in H^r(\Omega)$ with $r > 1$, then there exists $C > 0$ independent of $N$ and $H$ such that

$$\|u - u_{\mathcal{H}}\|_{H^1(\Omega)} \leq C \left[ H^{\min(N+1,s)-1} N^{1-s} \|u\|_{H^s(\Omega)} + H^{\min(N+1,r)} N^{-r} \|f\|_{H^r(\Omega)} \right]. \tag{103}$$

The proof follows by the application of theorem 1.2, lemma 1.3 and by the following approximation result of Babuska and Suri [4]:

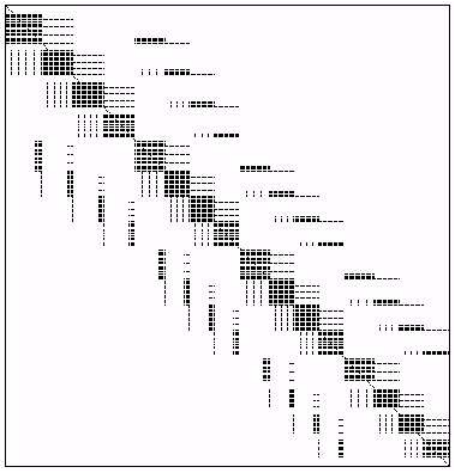

Figure 2: The pattern of the matrix $A_{\mathcal{H}}$ on a decomposition in $4\times 4$ spectral elements with $N = 4$.

**Theorem 1.4** Let $u \in H^s(\Omega) \cap H_0^1(\Omega)$, with $s > 3/2$, then for any $N \geq 1$ and $H > 0$ there exists $z_{\mathcal{H}} \in V_{\mathcal{H}}$ such that

$$\|u - z_{\mathcal{H}}\|_{H^k(\Omega)} \leq C H^{\min(N+1,s)-k} N^{k-s} \|u\|_{H^s(\Omega)} \qquad k = 0, 1 \tag{104}$$

where $C$ is independent of $u$, $N$, $H$ and $\mathcal{T}_H$. □

Consider now the algebraic form of problem (99). The matrix $A_{\mathcal{H}}$ associated to the bilinear form

$$a_{\mathcal{H}}(u_{\mathcal{H}}, v_{\mathcal{H}}) = \sum_{k=1}^{Ne} a_{N,k}(u_{N,k}, v_{N,k}) \tag{105}$$

has a sparse structure. An example of $A_{\mathcal{H}}$ for a domain which is split into $4 \times 4$ elements with polynomials of degree $N = 4$ is shown in Fig. 2.

From numerical experiments we obtained that the condition number of the Spectral Element matrix is

$$\chi(A_{\mathcal{H}}) \leq C N^3 H^{-2}. \tag{106}$$

The sparsity of the matrix and the high dependence of the condition number by the discretization parameters $N$ and $H$ suggest to solve the linear system $A_{\mathcal{H}}\mathbf{u} = \mathbf{f}$ associated to (99) by preconditioned Krylov Methods. An optimal preconditioner for this system can be provided by the global bilinear finite element matrix (see the Remark in Sec. 4.1). Another is given by the inexact additive Schwarz method with coarse correction ([27], [28], [60], [32]), that we briefly describe hereafter.

Consider a decomposition of the computational domain $\Omega$ in $Ne$ conformal non-overlapping spectral elements $T_k$ and a coarse mesh $\mathcal{M}_0$ given by the vertices of all the elements $T_k$. Then, for any $T_k \in \mathcal{T}_H$, consider an extension $T_{k,e}$ overlapping the adjacents elements of one or two nodes in each direction and the fine mesh $\mathcal{M}_{k,e}$ of all Legendre Gauss-Lobatto nodes in $T_{k,e}$ (see Fig. 3).

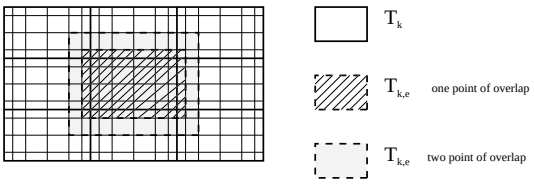


Figure 3: The spectral elements $T_k$ and the extended elements $T_{k,e}$ with one or two nodes of overlap.

Let $A_0$ (resp. $A_{k,e}$) be the bilinear finite (or spectral) element matrix associated to the discretization of the problem (2) on the mesh $\mathcal{M}_0$ (resp. $\mathcal{M}_{k,e}$). Let $R_0^T$ (resp. $R_{k,e}^T$) be the extension matrix whose action extends to zero a vector of nodal values in $\mathcal{M}_0$ (resp. in $\mathcal{M}_{k,e}$). The transposes $R_0$ and $R_{k,e}$ are restrictions matrices whose action restricts a full vector defined on all the nodes in $\Omega$ to a local vector on $\mathcal{M}_0$ or $\mathcal{M}_{k,e}$.
The inexact additive Schwarz preconditioner $P_{as}$ for $A_{\mathcal{H}}$ with coarse refinement is defined as follows:

$$P_{as}^{-1} := R_0^T A_0^{-1} R_0 + \sum_{k=1}^{Ne} R_{k,e}^T A_{k,e}^{-1} R_{k,e}. \tag{107}$$

The attribute "inexact" to the preconditioner refers to the fact that the local matrices $A_{k,e}$ and the coarse matrix $A_0$ arise from bilinear finite (or spectral) element discretization rather than on the primary spectral element discretization directly. If finite element methods were used for both the primary discretization and the preconditioner, Driya and Widlund ([28], [27]) proved that $\exists C > 0$ independent of $H$ and $h$ (the size of the fine meshes on $T_{k,e}$), but possibly depending on $\nu$ such that:

$$\chi(P_{as}^{-1} A) \leq C(\nu)(1 + \beta^{-1}), \tag{108}$$

$A$ being the finite element matrix associated to the primary discretization and $\beta H$ the maximum extension of the elements $T_{k,e}$ along the $x_1$ or $x_2$ direction. For large jumps on the coefficient $\nu$ at the interface, the convergence rate can deteriorate and precisely $\exists C > 0$ independent of $H$, $h$ and $\nu$, but depending on $\beta$ such that

$$\chi(P_{as}^{-1} A) \leq C(\beta) \left(1 + \log \frac{H}{h}\right). \tag{109}$$

We come back now to spectral element approximation. An estimate similar to (108) holds also if we consider the matrix $A_{\mathcal{H}}$ instead of $A$, thanks to the equivalence of the two discretizations (see [15]). If we consider a decomposition in squared elements with $H_k = H$ for any $T_k \in \mathcal{T}_H$ and if we measure the extension of an element $T_k$ by mesh nodes and the extension amounts of one node in each direction, it follows that the overlap is $\beta H \simeq H/N^2$, i.e. the distance between the Legendre Gauss-Lobatto endpoint and the nearest one. The immediate consequence is that the condition number of the precondioned matrix $P_{as}^{-1} A_{\mathcal{H}}$ is bounded uniformly with respect to $H$ but not with respect to the polynomial degree $N$. In particular:

$$\chi(P_{as}^{-1} A_{\mathcal{H}}) \leq C(\nu)(1 + N^2), \tag{110}$$

| | | $M_1$ | | | | | | | | | |
|---|---|---|---|---|---|---|---|---|---|---|---|
| | | 2 | 3 | 4 | 5 | 6 | 7 | 8 | 9 | 10 | 11 |
| | 3 | 9 | 13 | 16 | 18 | 17 | 19 | 19 | 19 | 19 | 19 |
| | 4 | 9 | 13 | 15 | 16 | 15 | 16 | 16 | 16 | 16 | 16 |
| | 5 | 11 | 15 | 17 | 17 | 17 | 18 | 17 | 17 | 17 | 17 |
| $N$ | 6 | 12 | 15 | 17 | 17 | 17 | 18 | 18 | 18 | 18 | 18 |
| | 7 | 14 | 16 | 15 | 16 | 16 | 16 | 16 | 16 | 16 | 16 |
| | 8 | 14 | 15 | 17 | 17 | 15 | 15 | 15 | 16 | 16 | 16 |
| | 9 | 16 | 17 | 17 | 16 | 16 | 16 | 16 | 18 | 18 | 18 |

Table 1: The number of conjugate gradient iterations for the additive Schwarz preconditioner with coarse correction for the problem (112) with a decomposition of $\Omega$ in $M_1 \times M_1$ equal subdomains and one point of overlap.

for mild variations of $\nu$, and

$$\chi(P_{as}^{-1} A_{\mathcal{H}}) \leq C(\beta)(1 + \log(HN^2)), \tag{111}$$

in the case of severe discontinuities across the interfaces.

Since iterative methods are used, the matrices $A_{\mathcal{H}}$ and $P_{as}^{-1}$ are never explicitly assembled; a matrix-vector product involving $A_{\mathcal{H}}$ is performed by local matrix-vector products. Then (107) yields only local systems (for the matrices $A_{k,e}$), or the coarse system (for $A_0$), and all of them have relatively little dimension.
Let us show the number of conjugate gradient iterations preconditioned by the matrix $P_{as}^{-1}$ to solve with a tolerance $\epsilon = 10^{-6}$ the following problem:

$$\begin{cases} -\Delta u = f & \text{in } \Omega = (0,1)^2 \\ u = g & \text{on } \partial\Omega, \end{cases} \tag{112}$$

where $f$ and $g$ are fixed in a way that the exact solution is $u(\mathbf{x}) = e^{x_1+x_2}$. We have considered a decomposition of $\Omega$ into $Ne = M_1 \times M_1$ equal subdomains. The results refer to the overlap involving only one grid point outside each subdomain.

## 2 Stokes and Navier-Stokes equations

Given an open bounded domain $\Omega \subset \mathbb{R}^2$ and a time interval $(0,T)$, the Navier Stokes equations for Newtonian, viscous incompressible fluids read:

$$\begin{cases} \dfrac{\partial \mathbf{u}}{\partial t} - \nu\Delta\mathbf{u} + \nabla p = \mathbf{f} - (\mathbf{u}\cdot\nabla)\mathbf{u} & \text{in } \Omega \times (0,T) \\ \nabla \cdot \mathbf{u} = 0 & \text{in } \Omega \times (0,T) \\ \mathbf{u} = \mathbf{0} & \text{on } \partial\Omega \times (0,T) \\ \mathbf{u} = \mathbf{u}_0 & \text{in } \Omega \times \{0\}, \end{cases} \tag{113}$$

where $\nu$ is the kinematic viscosity, $\mathbf{u} = \mathbf{u}(\mathbf{x},t)$ is the velocity field, $p = p(\mathbf{x},t)$ is the kinematic pressure, $\mathbf{u}_0 = \mathbf{u}_0(\mathbf{x})$ and $\mathbf{f} = \mathbf{f}(\mathbf{x},t)$ are the initial data and the external force field, respectively.

| | | $M_1$ | | | | | | | | | |
|---|---|---|---|---|---|---|---|---|---|---|---|
| | | 2 | 3 | 4 | 5 | 6 | 7 | 8 | 9 | 10 | 11 |
| | 2 | 5 | 15 | 18 | 21 | 24 | 26 | 26 | 27 | 27 | 27 |
| | 3 | 10 | 16 | 23 | 25 | 27 | 27 | 27 | 28 | 28 | 28 |
| | 4 | 12 | 16 | 22 | 23 | 24 | 24 | 24 | 23 | 24 | 23 |
| | 5 | 13 | 15 | 19 | 21 | 21 | 21 | 21 | 21 | 21 | 21 |
| $N$ | 6 | 12 | 16 | 19 | 19 | 20 | 20 | 19 | 20 | 20 | 20 |
| | 7 | 12 | 15 | 16 | 18 | 18 | 18 | 18 | 18 | 17 | 17 |
| | 8 | 13 | 16 | 15 | 17 | 16 | 16 | 16 | 16 | 16 | 16 |
| | 9 | 14 | 16 | 16 | 16 | 16 | 16 | 16 | 16 | 16 | 16 |

Table 2: The number of conjugate gradient iterations for the additive Schwarz preconditioner with coarse correction for the problem (112) with a decomposition of $\Omega$ in $M_1 \times M_1$ equal subdomains and two points of overlap.

Before analysing the Navier-Stokes system and its discretization in time, we want to face up the discretization of the generalized Stokes problem, since many time-differentiation algorithms for the Navier-Stokes system can be reduced to a successive resolution of generalized Stokes systems.

## 2.1 Analysis of the generalized Stokes problem

The generalized Stokes equations read:

$$\begin{cases} \alpha \mathbf{u} - \nu \Delta \mathbf{u} + \nabla p = \mathbf{f} & \text{in } \Omega \\ \nabla \cdot \mathbf{u} = 0 & \text{in } \Omega \\ \mathbf{u} = 0 & \text{on } \partial\Omega, \end{cases} \tag{114}$$

with $\mathbf{f} \in [L^2(\Omega)]^2$ and $\alpha$ is a non-negative constant. Given

$$\mathbf{V} = \left[H_0^1(\Omega)\right]^2 \text{ and } \qquad Q = L_0^2(\Omega) = \left\{ q \in L^2(\Omega : \int_\Omega q \mathrm{d}\Omega = 0 \right\}, \tag{115}$$

the weak formulation of (114) reads: find $\mathbf{u} \in \mathbf{V},\ p \in Q$ :

$$\begin{cases} a(\mathbf{u}, \mathbf{v}) + b(\mathbf{v}, p) = (\mathbf{f}, \mathbf{v})_{L^2(\Omega)} & \forall \mathbf{v} \in \mathbf{V} \\ b(\mathbf{u}, q) = 0 & \forall q \in Q, \end{cases} \tag{116}$$

with

$$\begin{aligned} a(\mathbf{u}, \mathbf{v}) &= \int_\Omega \nu \nabla \mathbf{u} \cdot \nabla \mathbf{v} d\Omega + \int_\Omega \alpha \mathbf{u} \cdot \mathbf{v} d\Omega, \\ b(\mathbf{v}, q) &= -\int_\Omega q \nabla \cdot \mathbf{v} d\Omega. \end{aligned} \tag{117}$$

When the Stokes (or Navier-Stokes) equations in the primitive variable formulation are approximated by Galerkin methods, a compatibility condition between the finite dimensional spaces for velocity and pressure has to be satisfied.
As a matter of fact, when the continuity equation is discretized directly, some parasitic modes on the pressure can appear with a deterioration of the accuracy on the numerical solution. The parasitic modes have been characterised mathematically for equal order polynomial approximation of velocity and pressure. Various techniques have been developed in order to filter them out. We give a short account hereafter.

We consider the generalized Galerkin approach (see Sec. 1.4) in order to approximate (116): find $\mathbf{u}_N \in \mathbf{V}_N \subset \mathbf{V},\ p_N \in Q_N \subset Q$ :

$$\begin{cases} a_N(\mathbf{u}_N, \mathbf{v}_N) + b_N(\mathbf{v}_N, p_N) = (\mathbf{f}, \mathbf{v}_N)_{N,\Omega} & \forall \mathbf{v}_N \in \mathbf{V}_N \\ b_N(\mathbf{u}_N, q_N) = 0 & \forall q_N \in Q_N, \end{cases} \tag{118}$$

with

$$\begin{aligned} a_N(\mathbf{u}_N, \mathbf{v}_N) &= (\nu \nabla \mathbf{u}_N, \nabla \mathbf{v}_N)_{N,\Omega} + (\alpha \mathbf{u}_N, \mathbf{v}_N)_{N,\Omega} \\ b_N(\mathbf{v}_N, q_N) &= -(q_N, \nabla \cdot \mathbf{v}_N)_{N,\Omega}, \end{aligned} \tag{119}$$

and where $\mathbf{V}_N$ and $Q_N$ are finite dimensional polynomial subspaces of $\mathbf{V}$ and $Q$ respectively.

The space of parasitic modes for the pressure, i.e. the elements of the following space:

$$Z_N = \{q_N \in Q_N :\ b_N(\mathbf{v}_N, q_N) = 0,\ \forall \mathbf{v}_N \in \mathbf{V}_N\}, \tag{120}$$

is empty if and only if the following *inf-sup* or *Ladyzenskaya-Brezzi-Babuška (LBB)* condition is satisfied (see [2], [12]):

$$\exists \beta > 0 :\ \forall q_N \in Q_N\ \exists \mathbf{v}_N \in V_N :\quad b_N(\mathbf{v}_N, q_N) \geq \beta \|\mathbf{v}_N\|_{H^1(\Omega)} \|q_N\|_{L^2(\Omega)}. \tag{121}$$

The a priori most obvious choice

$$\mathbf{V}_N = \left[\mathbb{Q}_N(\Omega) \cap H_0^1(\Omega)\right]^2 \text{ and } Q_N = \mathbb{Q}_N(\Omega) \cap L_0^2(\Omega) \tag{122}$$

gives $\dim Z_N = 7$, with

$$Z_N = span\{L_N(x),\ L_N(y),\ L_N(x)L_N(y),\ L'_N(x)L'_N(y)(1 \pm x)(1 \pm y)\}. \tag{123}$$

Should the Chebyshev (rather than Legendre) Gauss-Lobatto quadrature be used, the space $Z_N$ would have a similar characterisation, with the Chebyshev polynomials $T_N$ instead of $L_N$. See [5].

The parasitic modes can be filtered out, for example, by a transform from the physical space to the frequency space, projecting $p_N$ upon the space $Z_N^{\perp}$, and then by anti-transforming to the physical space.

Another strategy consists of choosing $\mathbf{V}_N$ as before and $Q_N$ satisfying (see [5]):

$$\begin{aligned} &Q_N \oplus Z_N = \mathbb{Q}_N(\Omega) \cap L_0^2(\Omega), \qquad\qquad Q_N \cap Z_N = \{0\}, \\ &\dim Q_N + \dim Z_N = \dim(\mathbb{Q}_N(\Omega) \cap L_0^2(\Omega)). \end{aligned} \tag{124}$$

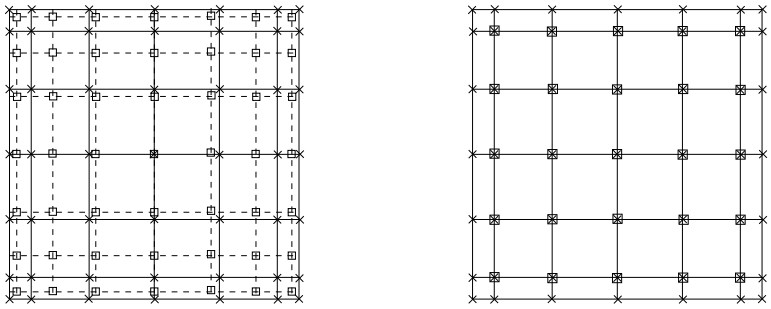

Figure 4: At left the two staggered grids: Legendre Gauss-Lobatto ($\times$) for the velocity and Legendre Gauss ($\square$) for the pressure. At right the two grids: Legendre Gauss-Lobatto ($\times$) for the velocity and internal Legendre Gauss-Lobatto ($\square$) for the pressure

In this case, the ($LBB$) condition (121) is satisfied with a constant $\beta = \beta_N = \mathcal{O}(N^{-1})$ and, if $\mathbf{u} \in H^{s+1}(\Omega)$, $p \in H^s(\Omega)$, the following error estimate holds:

$$\|\mathbf{u} - \mathbf{u}_N\|_{H^1(\Omega)} + N^{-1}\|p - p_N\|_{L^2(\Omega)} \leq CN^{-s}\left(\|\mathbf{u}\|_{H^{s+1}(\Omega)} + \|p\|_{H^s(\Omega)}\right). \tag{125}$$

Due to the difficulty to build the space $Q_N$, the interest of this choice is more theoretical than practical.
A more practical choice from the computational viewpoint is to take

$$Q_N = \mathbb{Q}_{N-2}(\Omega) \cap L^2_0(\Omega). \tag{126}$$

The ($LBB$) condition (121) is satisfied with $\beta = \beta_N = \mathcal{O}(N^{-1/2})$, and (see [50])

$$\begin{aligned} \|\mathbf{u} - \mathbf{u}_N\|_{H^1(\Omega)} + N^{-1/2}\|p - p_N\|_{L^2(\Omega)} \leq \\ CN^{-s}\left(\|\mathbf{u}\|_{H^{s+1}(\Omega)} + \|p\|_{H^s(\Omega)}\right). \end{aligned} \tag{127}$$

Two ways can be followed in order to implement this approach. The former consists in using a staggered grid, a Legendre Gauss-Lobatto grid for the velocity and a Legendre Gauss grid for the pressure (as in Fig. 4, left); in this way an interpolation process is needed in order to compute the values for $\nabla p_N$ on the velocity grid. Alternatively, one can use for the pressure the $(N-1)^2$ Legendre Gauss-Lobatto quadrature nodes internal to the computational domain (see Fig. 4, right); the incompressibility condition is enforced by a discrete quadrature formula which is no more a Gaussian quadrature formula ([5]).

An alternative approach to those mentioned above is to use equal order interpolation spaces (122) and consequently stabilize the Stokes equations *à la* Galerkin Least Squares, or *à la* Douglas-Wang (see [40], [39]).

The stabilization techniques, initially proposed in the finite element context, have then been extended to spectral methods (see [17], [61]) and the spectral element methods (see [34]) with a suitable design of the stabilization parameters.
We briefly describe the stabilization *à la* Douglas-Wang on the spectral element

approximation of (118). It consists of finding $\mathbf{u}_N$ and $p_N$ in the spaces (122), such that:

$$\begin{aligned} a_N(\mathbf{u}_N,\mathbf{v}_N) + b_N(\mathbf{v}_N,p_N) - b_N(\mathbf{u}_N,q_N) & \\ +(\alpha\mathbf{u}_N - \nu\Delta\mathbf{u}_N + \nabla p_N, \tau(\alpha\mathbf{v}_N - \nu\Delta\mathbf{v}_N + \nabla q_N))_{N,\Omega} & \\ = (\mathbf{f}, \tau(\alpha\mathbf{v}_N - \nu\Delta\mathbf{v}_N + \nabla q_N))_{N,\Omega} & \\ \forall \mathbf{v}_N \in \mathbf{V}_N, \quad \forall q_N \in Q_N, & \end{aligned} \tag{128}$$

where $\tau$ is the stabilization parameter which depends on the viscosity $\nu$, on the domain size, and on the polynomial degree. A particular choice for $\tau$ is

$$\tau = \frac{m \ \mathrm{meas}(\Omega)}{N^4}, \tag{129}$$

The bilinear form

$$\begin{aligned} \mathcal{B}_N(\mathbf{u}_N,p_N;\mathbf{v}_N,q_N) := \quad & a_N(\mathbf{u}_N,\mathbf{v}_N) + b_N(\mathbf{v}_N,p_N) - b_N(\mathbf{u}_N,q_N) \\ & +(\alpha\mathbf{u}_N - \nu\Delta\mathbf{u}_N + \nabla p_N, \tau(\alpha\mathbf{v}_N - \nu\Delta\mathbf{v}_N + \nabla q_N))_{N,\Omega}, \end{aligned} \tag{130}$$

associated to the approximation (128), is coercive with a coercivity constant equal to one. Consequently the solution satisfy the following stability inequality: $\exists\beta > 0$ independent of $N$ such that

$$|||[\mathbf{u}_N,p_N]|||_\Omega \leq \beta \|\mathbf{f}\|_{N,\Omega} \tag{131}$$

where

$$\begin{aligned} |||[\mathbf{u}_N,p_N]|||_\Omega := \quad & \Big(\alpha\|\mathbf{u}_N\|^2_{L^2(\Omega)} + \nu\|\nabla\mathbf{u}_N\|^2_{L^2(\Omega)} \\ & +\|\tau^{1/2}(\alpha\mathbf{u}_N - \nu\Delta\mathbf{u}_N + \nabla p_N)\|^2_{L^2(\Omega)}\Big)^{1/2}. \end{aligned} \tag{132}$$

Furthermore, the solution of (128) satisfies the following error estimate: if the solution of (116) is such that $\mathbf{u} \in H^s(\Omega),\ s \geq 2, p \in H^l(\Omega),\ l \geq 1$ and $\mathbf{f} \in H^r(\Omega),\ r > 1$, then there exists a positive constant $C$ independent of $N$ such that

$$|||[\mathbf{u}-\mathbf{u}_N,p-p_N]|||_\Omega \leq C\left[N^{1-s}\|\mathbf{u}\|_{H^s(\Omega)} + N^{-l}\|p\|_{H^l(\Omega)} + N^{-r}\|\mathbf{f}\|_{H^r(\Omega)}\right]. \tag{133}$$

Other stabilization approaches are possible, for instance based on *streamline upwind Galerkin* methods, or else on the *bubble stabilized spectral* method proposed by Canuto and Van-Kemenade ([17]). Stabilization methods for the so-called $hp-$FEM are analyzed in [75] and [76].

# 3 Time-differentiation of Navier Stokes equations

We focus now our attention on the discretization of the temporal derivative in (113) and review some of the schemes which have been more successfully used in the past years.

### 3.1 Finite difference schemes

The most classical approach consists in advancing in time by suitable explicit, implicit or semi-implicit finite difference schemes.
The explicit schemes are easy to implement, the basic computational kernel required is a matrix-vector product, but an obvious restriction on the choice of the time step is needed to ensure stability to the scheme.

On the other hand, a fully implicit scheme requires the solution of a non-linear system at every time step, but no bounds on the time step are needed.
One way to avoid the resolution of a non-linear system is to use semi-implicit methods in which the nonlinear convective term is replaced by a linearised one. An example is provided by the Euler semi-implicit scheme that reads as follows. Given $\Delta t \in (0,T)$ we set $t^0 = 0$ and $t^n = t^0 + n \cdot \Delta t$ with $n = 1, .., \mathcal{N}$ and $\mathcal{N} = \left[\frac{T}{\Delta t}\right]$ (where $[a]$ stands for integral part of $a$). Then, for $n = 0, ..., \mathcal{N} - 1$, find $[\mathbf{u}^{n+1}, p^{n+1}] \in \mathbf{V} \times Q$ :

$$\begin{cases} \dfrac{\mathbf{u}^{n+1} - \mathbf{u}^n}{\Delta t} - \nu \Delta \mathbf{u}^{n+1} + \nabla p^{n+1} = \mathbf{f}^{n+1} - (\mathbf{u}^n \cdot \nabla)\mathbf{u}^{n+1} & \text{in } \Omega \\ \nabla \cdot \mathbf{u}^{n+1} = 0 & \text{in } \Omega. \end{cases} \tag{134}$$

Otherwise the non linear terms can be treated fully explicitly, and the other ones fully implicitly as in the Crank-Nicolson/Adams-Bashforth (CN-AB) second order scheme, that, on system (113), reads as follows:

$$\begin{cases} \dfrac{\mathbf{u}^{n+1} - \mathbf{u}^n}{\Delta t} - \dfrac{\nu}{2}\Delta(\mathbf{u}^{n+1} + \mathbf{u}^n) + \dfrac{1}{2}\nabla(p^{n+1} + p^n) = \\ \quad \dfrac{1}{2}(\mathbf{f}^{n+1} + \mathbf{f}^n) - \dfrac{1}{2}\left[3(\mathbf{u}^n \cdot \nabla)\mathbf{u}^n - (\mathbf{u}^{n-1} \cdot \nabla)\mathbf{u}^{n-1}\right] & \text{in } \Omega \\ \nabla \cdot \mathbf{u}^{n+1} = 0 & \text{in } \Omega \end{cases} \tag{135}$$

with a suitable second order approximation of $\mathbf{u}^1$. At each time step a generalized Stokes problem as (114) has to be solved. If the spectral collocation method is used for space discretization, this method is stable under the condition that $\Delta t \leq CN^{-2}$.
Another semi-implicit scheme is based on the second-order backward finite-difference formula (see [37]):

$$\begin{cases} \dfrac{3\mathbf{u}^{n+1} - 4\mathbf{u}^n + \mathbf{u}^{n-1}}{2\Delta t} - \nu \Delta \mathbf{u}^{n+1} + \nabla p^{n+1} = \\ \quad \mathbf{f}^{n+1} - \left((2\mathbf{u}^n - \mathbf{u}^{n-1}) \cdot \nabla\right)(2\mathbf{u}^n - \mathbf{u}^{n-1}) & \text{in } \Omega \\ \nabla \cdot \mathbf{u}^{n+1} = 0 & \text{in } \Omega. \end{cases} \tag{136}$$

Also in this case at each time step a generalized Stokes problem has to be solved.

We refer also to Simo and Armero (see [79]) for other finite difference schemes of various order, explicit, implicit or semi-implicit, with very-good stability properties in time, that may be applied to spectral approximation. In particular, a second

order accurate algorithm that retains the key property of unconditional stability and linearity within the time step, reads

$$\begin{cases} \dfrac{\mathbf{u}^{n+1}-\mathbf{u}^n}{\Delta t} - \dfrac{\nu}{2}\Delta(\mathbf{u}^{n+1}+\mathbf{u}^n) + \nabla p^{n+1} = \\ \quad \dfrac{1}{2}(\mathbf{f}^{n+1}+\mathbf{f}^n) - \dfrac{1}{4}\left[(3\mathbf{u}^n - \mathbf{u}^{n-1})\cdot\nabla(\mathbf{u}^{n+1}+\mathbf{u}^n)\right] & \text{in } \Omega \\ \nabla\cdot(\mathbf{u}^{n+1}+\mathbf{u}^n) = 0 & \text{in } \Omega. \end{cases} \tag{137}$$

Now we show how to combine finite difference schemes for time-discretization with space-stabilized Galerkin methods. As an instance, we use the Euler semi-implicit scheme (134) for the Douglas-Wang stabilization method that was formerly used in (128) on the Stokes problem (114) (we refer to [34] for a more detailed description and analysis). For $n = 0, ..., \mathcal{N}-1$, find $[\mathbf{u}_N^{n+1}, p_N^{n+1}] \in \mathbf{V}_N \times Q_N$ :

$$\begin{aligned} &\frac{1}{\Delta t}(\mathbf{u}_N^{n+1}-\mathbf{u}_N^n, \mathbf{v}_N)_{N,\Omega} + a_N(\mathbf{u}_N^{n+1}, \mathbf{v}_N) + b_N(\mathbf{u}_N^{n+1}, q_N) \\ &\quad + c_N(\mathbf{u}_N^n, \mathbf{u}_N^{n+1}, \mathbf{v}_N) + b_N(\mathbf{v}_N, p_N^{n+1}) + (\nabla\cdot\mathbf{u}_N^{n+1}, \gamma(\mathbf{x})\nabla\cdot\mathbf{v}_N)_{N,\Omega} \\ &\quad + \left(\frac{\mathbf{u}_N^{n+1}}{\Delta t} + L(\mathbf{u}_N^n, \mathbf{u}_N^{n+1}, p_N^{n+1}), \tau(\mathbf{x})L(\mathbf{u}_N^n, \mathbf{v}_N, q_N)\right)_{N,\Omega} = \\ &\quad = (\mathbf{f}^{n+1}, \mathbf{v}_N)_{N,\Omega} + \left(\mathbf{f}^{n+1} + \frac{\mathbf{u}_N^n}{\Delta t}, \tau(\mathbf{x})L(\mathbf{u}_N^n, \mathbf{v}_N, q_N)\right)_{N,\Omega} \\ &\qquad\qquad \forall \mathbf{v}_N \in \mathbf{V}_N,\ q_N \in Q_N \end{aligned} \tag{138}$$

with $\mathbf{u}_N^0 = \mathbf{u}_{0_N}$, where

$$L(\mathbf{w}, \mathbf{u}, p) = -\Delta\mathbf{u} + (\mathbf{w}\cdot\nabla)\mathbf{u} + \nabla p, \tag{139}$$

and

$$c_N(\mathbf{w}_N, \mathbf{u}_N, \mathbf{v}_N) = ((\mathbf{w}_N\cdot\nabla)\mathbf{u}_N, \mathbf{v}_N)_{N,\Omega},\ \forall \mathbf{w}_N, \mathbf{u}_N, \mathbf{v}_N \in \mathbf{V}_N. \tag{140}$$

We observe that if in (138) we put $q_N = 0$ then we obtain the stabilized momentum equation, while, if we put $\mathbf{v}_N = 0$ we obtain the stabilized continuity equation.

The stabilization parameters $\tau(\mathbf{x})$ and $\gamma(\mathbf{x})$ can be defined as follows:

$$\tau(\mathbf{x}) = \frac{\text{meas}(\Omega)}{2|\mathbf{u}_N^n(\mathbf{x})|_p N^2}\xi(Re(\mathbf{x})), \qquad \gamma(\mathbf{x}) = \frac{\lambda|\mathbf{u}_N^n(\mathbf{x})|_p\,\text{meas}(\Omega)}{N^2}\xi(Re(\mathbf{x})), \tag{141}$$

where:

$$Re(\mathbf{x}) = \frac{m|\mathbf{u}_N^n(\mathbf{x})|_p\,\text{meas}(\Omega)}{2\nu N^2}, \quad \xi(Re(\mathbf{x})) = \begin{cases} Re(\mathbf{x}) & \text{if } 0 \le Re(\mathbf{x}) < 1 \\ 1 & \text{if } 1 \le Re(\mathbf{x}), \end{cases} \tag{142}$$

$$|\mathbf{u}_N^n(\mathbf{x})|_p = \begin{cases} (|(\mathbf{u}_N^n)_1(\mathbf{x})|^p + |(\mathbf{u}_N^n)_2(\mathbf{x})|^p)^{1/p} & \text{if } 1 \le p < \infty \\ \max\limits_{i=1,2}|(\mathbf{u}_N^n)_i(\mathbf{x})| & \text{if } p = \infty. \end{cases} \tag{143}$$

For each $n = 0, .., \mathcal{N}$ there exists a unique solution of (138). Moreover, if $\mathbf{u} \in [H_0^1(\Omega) \cap H^{s+1}(\Omega)]^2$ with $s \geq 1$, $p \in L_0^2(\Omega) \cap H^l(\Omega)$ with $l \geq 1$, $\mathbf{w} \in W^{\max(s,l,r),\infty}(\Omega)$, $\mathbf{f} \in H^r(\Omega)$ with $r > 1$, then there exists a positive constant $C$ independent of $N$ such that:

$$|||[\mathbf{u} - \mathbf{u}_N, p - p_N]|||_\Omega \leq C\Big(N^{1-s}\|\mathbf{u}\|_{H^s(\Omega)} + N^{-l}\|p\|_{H^l(\Omega)} + N^{-r}\|\mathbf{f}\|_{H^r(\Omega)}\Big). \quad (144)$$

Another possible choice for $\tau$ and $\gamma$ is given in [17], where $\tau$ is locally defined on each quadrilateral $T_k$ arising from the Legendre Gauss-Lobatto grid in the following way:

$$\tau_k(\mathbf{x}) = \frac{h_k}{2|\mathbf{u}_N^n(\mathbf{x})|_p}\xi(Re_k(\mathbf{x})), \quad (145)$$

$$\xi(Re_k(\mathbf{x})) = \begin{cases} \dfrac{mh_k|\mathbf{u}_N^n(\mathbf{x})|_p}{4\nu} & \text{if } 0 \leq Re_k(\mathbf{x}) \leq 1 \\ 1 & \text{if } Re_k(\mathbf{x}) > 1, \end{cases} \quad (146)$$

with

$$h_k = \sqrt{2}\frac{\text{meas}(k)}{\text{diag}(k)} \qquad \text{or} \qquad h_k = h_{k_x}\cos\theta + h_{k_y}\sin\theta \quad (147)$$

and

$$\theta = \arctan(|\mathbf{u}_{N,2}^n|/|\mathbf{u}_{N,1}^n|), \quad (148)$$

while $\gamma$ is taken equal to zero. This strategy is more sensible to local changes of the ratio $|\mathbf{u}_N|/\nu$ than the former one (141).

We notice that in (138) the velocity components are unfortunally coupled through the term $(\nabla \cdot \mathbf{u}_N^{n+1}, \gamma(\mathbf{x})\nabla \cdot \mathbf{v}_N)_{N,\Omega}$, whose presence is necessary in order to prove the stability of the numerical solution.

## 3.2 Projection methods

The idea of these schemes, introduced by Chorin (1968) and Temam (1969) consists in decoupling the resolution of the velocity and the pressure in order to overcome the incompressibility constraint $\nabla \cdot \mathbf{u} = 0$.
First, a non-linear elliptic advection-diffusion problem of the following form

$$\begin{cases} \dfrac{\tilde{\mathbf{u}}^{n+1} - \mathbf{u}^n}{\Delta t} - \nu\Delta\tilde{\mathbf{u}}^{n+1} + B(\tilde{\mathbf{u}}^{n+\alpha}, \tilde{\mathbf{u}}^{n+\beta}) = \dfrac{1}{\Delta t}\displaystyle\int_{t_n}^{t_{n+1}} \mathbf{f}(t)dt & \text{in } \Omega \\ \tilde{\mathbf{u}}^{n+1} = 0 & \text{on } \partial\Omega, \end{cases} \quad (149)$$

is solved, where $B(\mathbf{u}, \mathbf{v}) = (\mathbf{u} \cdot \nabla)\mathbf{v} + 1/2(\nabla \cdot \mathbf{u})\mathbf{v}$ is the skew-symmetric form of the non-linear term, $\alpha,\ \beta \in [0, 1]$. Therefore the numerical solution $\mathbf{u}^{n+1}$ is computed as the projection of $\tilde{\mathbf{u}}^{n+1}$ on the free-divergence space

$$\mathbf{V}_{\text{div}} = \{\mathbf{v} \in \mathbf{V} :\ \nabla \cdot \mathbf{v} = 0\} \quad (150)$$

with respect to the scalar product in $[L^2(\Omega)]^2$, i.e.

$$(\mathbf{u}^{n+1}, \mathbf{w})_{L^2(\Omega)} = (\tilde{\mathbf{u}}^{n+1}, \mathbf{w})_{L^2(\Omega)} \qquad \forall \mathbf{w} \in \mathbf{V}_{\text{div}}. \tag{151}$$

For the projection step (151) the method and all its variants are known as "projection methods".
As a consequence of the so-called Helmholtz decomposition principle ([71]), the computation of $\mathbf{u}^{n+1}$ by (151) is reduced to the resolution of an elliptic problem with Neumann boundary conditions for the pressure $p^{n+1}$:

$$\begin{cases} \Delta p^{n+1} = \dfrac{1}{\Delta t} \nabla \cdot \tilde{\mathbf{u}}^{n+1} & \text{in } \Omega \\ \dfrac{\partial p^{n+1}}{\partial \mathbf{n}} = 0 & \text{on } \partial\Omega, \end{cases} \tag{152}$$

from which we recover the end-of-step velocity field

$$\mathbf{u}^{n+1} = \tilde{\mathbf{u}}^{n+1} - \Delta t \nabla p^{n+1}. \tag{153}$$

Karniadakis et al. ([42], [78]) proposed a family of high-order time accurate splitting methods with improved boundary conditions of high order in time that minimize the effect of erroneous numerical boundary layers induced by splitting methods. The schemes read:

$$\begin{cases} \dfrac{\hat{\mathbf{u}} - \mathbf{u}^n}{\Delta t} = \displaystyle\sum_{j=0}^{J_e - 1} \beta_j (\mathbf{u}^{n-j} \cdot \nabla) \mathbf{u}^{n-j} & \text{in } \Omega \\ \dfrac{\hat{\hat{\mathbf{u}}} - \hat{\mathbf{u}}}{\Delta t} = -\nabla \overline{p}^{n+1} & \text{in } \Omega \\ \dfrac{\mathbf{u}^{n+1} - \hat{\hat{\mathbf{u}}}}{\Delta t} = \nu \displaystyle\sum_{j=0}^{J_p - 1} \gamma_j \Delta \mathbf{u}^{n+1-j} & \text{in } \Omega \end{cases} \tag{154}$$

with Dirichlet boundary conditions on $\mathbf{u}^{n+1}$. The incompressibility constraint is satisfied by the intermediate solution $\hat{\hat{\mathbf{u}}}$ and $\overline{p}^{n+1}$ is a scalar field that ensures that final velocity field is incompressible at the end of time level $(n+1)$. The coefficients $\beta_j$, for $j = 0, ..., J_e - 1$, and $\gamma_j$, for $j = 0, ..., J_p - 1$, can be the coefficients of Adams-Bashforth and Adams-Moulton methods (respectively of order $J_e$ and $J_p$), or more general multistep schemes. For other splitting methods see [16], Sec. 7.3.2.
Rannacher ([74]) has made a thorough analysis of the projection method and of its relation with stabilization methods (penalty methods). He has considered the following form of the projection method: for $n = 0, .., \mathcal{N} - 1$:

$$\begin{cases} \dfrac{\mathbf{u}^{n+1/2} - \mathbf{u}^{n-1/2}}{\Delta t} - \nu \Delta \mathbf{u}^{n+1/2} + B(\mathbf{u}^{n+1/2}, \mathbf{u}^{n+1/2}) & \\ \qquad + \nabla q^n = \dfrac{1}{\Delta t} \displaystyle\int_{t_n}^{t_{n+1}} \mathbf{f}(t) dt & \text{in } \Omega \\ \mathbf{u}^{n+1/2} = 0 & \text{on } \partial\Omega \end{cases} \tag{155}$$

then find $q^{n+1}$:

$$\begin{cases} \Delta q^{n+1} = \dfrac{1}{\Delta t}\nabla \cdot \mathbf{u}^{n+1/2} & \text{in } \Omega \\ \dfrac{\partial q^{n+1}}{\partial \mathbf{n}} = 0 & \text{on } \partial\Omega, \end{cases} \tag{156}$$

with $\mathbf{u}^{-1/2} = \mathbf{u}_0$, $q^0 = 0$ and $\{q^n\}$ a sequence approximating $\{p^n\}$.
The velocity and the pressure are proven to be convergent at the first order with respect to the norms of $[L^2(\Omega)]^2$ and of the dual space of $H^1(\Omega) \cap L^2_0(\Omega)$, respectively. The analysis of Rannacher indicates that in the interior of the computational domain $\Omega$ the pressure $q^n$ is indeed a reasonable approximation of the exact pressure $p$ at time $t_n$, as the effects of the non-physical Neumann boundary condition in (156) decay exponentially with respect to $dist(\mathbf{x}, \partial\Omega)\sqrt{\Delta t}$.

Shen ([77]) proposed the following scheme:

$$\begin{cases} \dfrac{\mathbf{u}^{n+1/2} - \mathbf{u}^n}{\Delta t} - \dfrac{\nu}{2}\Delta(\mathbf{u}^{n+1/2} + \mathbf{u}^n) + B\left(\dfrac{\mathbf{u}^{n+1/2} + \mathbf{u}^n}{2}, \dfrac{\mathbf{u}^{n+1/2} + \mathbf{u}^n}{2}\right) & \\ \qquad + \nabla p^n = \mathbf{f}(t_{n+1/2}) & \text{in } \Omega \\ \mathbf{u}^{n+1/2} + \mathbf{u}^n = 0 & \text{on } \partial\Omega, \end{cases} \tag{157}$$

$$\begin{cases} \Delta(p^{n+1} - p^n) = \dfrac{2}{\Delta t}\nabla \cdot \mathbf{u}^{n+1/2} & \text{in } \Omega \\ \dfrac{\partial p^{n+1}}{\partial \mathbf{n}} = \dfrac{\partial p^n}{\partial \mathbf{n}} & \text{on } \partial\Omega \end{cases} \tag{158}$$

and he proved that the scheme (157)-(158) is second order accurate in time for the velocity and at least first order accurate for the pressure. He proposed to use first-order accurate boundary conditions for the pressure as analysed by Karniadakis et al. ([42]) in the framework of spectral element approximation.

Pinelli et al. ([66]) use the Van Kan scheme ([41]) based on the CN-AB method (135):

$$\begin{cases} \dfrac{\tilde{\mathbf{u}}^{n+1} - \mathbf{u}^n}{\Delta t} - \dfrac{\nu}{2}\Delta(\tilde{\mathbf{u}}^{n+1} + \mathbf{u}^n) + \nabla p^n = \dfrac{1}{2}(\mathbf{f}_n + \mathbf{f}_{n+1}) & \\ \qquad -\dfrac{1}{2}(3B(\mathbf{u}^n, \mathbf{u}^n) - B(\mathbf{u}^{n-1}, \mathbf{u}^{n-1})) & \text{in } \Omega \\ \tilde{\mathbf{u}}^{n+1} = 0 & \text{on } \partial\Omega, \end{cases} \tag{159}$$

$$\begin{cases} \dfrac{1}{\Delta t}(\mathbf{u}^{n+1} - \tilde{\mathbf{u}}^{n+1}) + \dfrac{1}{2}\nabla(p^{n+1} - p^n) = 0 & \text{in } \Omega \\ \nabla \cdot \mathbf{u}^{n+1} = 0 & \text{in } \Omega. \end{cases} \tag{160}$$

Legendre collocation in two directions and Fourier expansion in the third direction are considered in order to simulate a turbulent flow in 3D. At each time level a Projection Decomposition solver (see Sec. 4) on the generalized Stokes problem is used on the directions approximated by Legendre collocation.

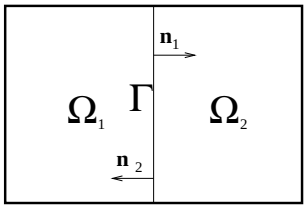


Figure 5: A decomposition of $\Omega$ in two subdomains.

# 4 Domain decomposition methods

The domain decomposition techniques are combined to the spectral methods for their good versatility to treat general geometries, as well as for the good properties that they enjoy as parallel preconditioners for the algebraic system arising from the spectral approximation.

Let us assume that $\Omega$ is partitioned into $M$ non-overlapping subdomains $\Omega_i$, $i = 1, ..., M$, such that $\overline{\Omega} = \cup_{i=1}^{M} \overline{\Omega}_i$. We set $\mathring{\Omega} = \cup_{i=1}^{M} \Omega_i$ and we define the interface between the subdomains as $\Gamma = \Omega \backslash \mathring{\Omega}$.

## 4.1 The Poisson problem

The first computational kernel used in the approximation of the Navier-Stokes equations is the Poisson problem

$$\begin{cases} -\Delta u = f & \text{in } \Omega \\ u = 0 & \text{on } \partial\Omega. \end{cases} \tag{161}$$

We indicate by $u_i$ the restriction to $\Omega_i$ of the solution $u$ to (161) and by $\mathbf{n}_i$ the outward unit normal vector to $\partial\Omega_i \cap \Gamma$.
For simplicity, we consider a rectangular domain $\Omega \subset \mathbb{R}^2$ split in two rectangular subdomains (see Fig. 5). For details and generalisation, see [72].
The multidomain formulation of (161) reads:

$$\begin{cases} -\Delta u_1 = f & \text{in } \Omega_1 \\ u_1 = 0 & \text{on } \partial\Omega_1 \cap \partial\Omega \\ u_1 = u_2 & \text{on } \Gamma \\ \dfrac{\partial u_1}{\partial \mathbf{n}_1} = -\dfrac{\partial u_2}{\partial \mathbf{n}_2} & \text{on } \Gamma \\ -\Delta u_2 = f & \text{in } \Omega_2 \\ u_2 = 0 & \text{on } \partial\Omega_2 \cap \partial\Omega. \end{cases} \tag{162}$$

The third and fourth equations of (162) are said transmission conditions for $u_1$ and $u_2$ and they ensure the necessary regularity of the multidomain solution.
The equivalence between (161) and (162) is shown by resorting to the weak form of both problems. The variational form of (161) reads:

$$\text{find } u \in V \equiv H_0^1(\Omega): \qquad a(u, v) = (f, v)_{L^2(\Omega)} \qquad \forall v \in V \tag{163}$$

with $a(u,v) = (\nabla u, \nabla v)_{L^2(\Omega)}$, while the variational multidomain form is: find $u_1 \in V_1,\ u_2 \in V_2$ :

$$\begin{cases} a_1(u_1, v_1) = (f, v_1)_{L^2(\Omega_1)} & \forall v_1 \in V_1^0 \\ a_2(u_2, v_2) = (f, v_2)_{L^2(\Omega_2)} & \forall v_2 \in V_2^0 \\ u_1 = u_2 & \text{on } \Gamma \\ a_2(u_2, E_2\mu) = (f, E_2\mu)_{L^2(\Omega_2)} - a_1(u_1, E_1\mu) + (f, E_1\mu)_{L^2(\Omega_1)} & \forall \mu \in \Lambda \end{cases} \tag{164}$$

where:

$$V_i = \{v_i \in H^1(\Omega_i) :\ v_i|_{\partial\Omega \cap \partial\Omega_i} = 0\} \qquad i = 1, 2, \tag{165}$$

($v_i|_\Gamma$ denotes the trace of $v_i$ on $\Gamma$),

$$V_i^0 = H_0^1(\Omega_i), \qquad i = 1, 2 \tag{166}$$

$$\Lambda = \{\mu \in H^{1/2}(\Gamma) :\ \mu = v|_\Gamma \text{ for a suitable } v \in V\}, \tag{167}$$

$$a_i(w_i, v_i) = (\nabla w_i, \nabla v_i)_{L^2(\Omega_i)} \qquad i = 1, 2 \tag{168}$$

and $E_i$ denotes any possible (continuous) operator from $\Lambda$ to $V_i$ which satisfies $(E_i\mu)|_\Gamma = \mu$, i.e. $E_i$ is an extension operator from $\Lambda$ to $V_i$.

The variational multidomain problem (164) can be equivalently written in terms of the Steklov Poincaré operator (see [1], [70]), where the determination of $u$, solution of (161) is reduced to find the trace $\lambda$ of $u$ on $\Gamma$ and then to solve $M$ independent Dirichlet problems on the subdomains $\Omega_i$.

As a matter of fact, we note that the solution $u$ to (162) can be represented as being $u = u_0 + v$, where $u_0$ is the solution to the following problems:

$$\begin{cases} -\Delta u_{0,i} = f & \text{in } \Omega_i \\ u_{0,i} = 0 & \text{on } \partial\Omega_i \end{cases} \qquad i = 1, 2 \tag{169}$$

(with $u_{0,i} = u_0|_{\Omega_i}$), while $v$ is the solution of

$$\begin{cases} -\Delta v_i = 0 & \text{in } \Omega_i \\ v_i = 0 & \text{on } \partial\Omega_i \cap \partial\Omega \\ v_i = \lambda & \text{on } \partial\Omega_i \cap \Gamma \end{cases} \qquad i = 1, 2 \tag{170}$$

(with $v_i = v|_{\Omega_i}$).
The equivalence with the original problem (162) is achieved provided that the following relation holds:

$$\frac{\partial u_1}{\partial \mathbf{n}_1} = -\frac{\partial u_2}{\partial \mathbf{n}_2} \qquad \text{on } \Gamma, \tag{171}$$

or:

$$\frac{\partial v_1}{\partial \mathbf{n}_1} + \frac{\partial v_2}{\partial \mathbf{n}_2} = -\left(\frac{\partial u_{0,1}}{\partial \mathbf{n}_1} + \frac{\partial u_{0,2}}{\partial \mathbf{n}_2}\right) \qquad \text{on } \Gamma. \tag{172}$$

Noticing that the functions $u_{0,i}$ only depend on $f$ (say $u_{0,i} = \mathcal{G}_i(f)$) and $v_i$ on $\lambda$ (say $v_i = \mathcal{H}_i(\lambda)$), we can formally write the equation (172) as:

$$\mathcal{S}\lambda = \chi \qquad \text{on } \Gamma \tag{173}$$

where

$$\chi = -\left(\frac{\partial u_{0,1}}{\partial \mathbf{n}_1} + \frac{\partial u_{0,2}}{\partial \mathbf{n}_2}\right) = -\left(\frac{\partial \mathcal{G}_1(f)}{\partial \mathbf{n}_1} + \frac{\partial \mathcal{G}_2(f)}{\partial \mathbf{n}_2}\right) \tag{174}$$

and

$$\mathcal{S}\lambda = \frac{\partial v_1}{\partial \mathbf{n}_1} + \frac{\partial v_2}{\partial \mathbf{n}_2} = \frac{\partial \mathcal{H}_1(\lambda)}{\partial \mathbf{n}_1} + \frac{\partial \mathcal{H}_2(\lambda)}{\partial \mathbf{n}_2}. \tag{175}$$

The equation (173) is said *interface equation* and $\mathcal{S}$ is the Steklov-Poincaré operator; $\mathcal{S}$ is self-adjoint and coercive.
To solve the interface equation amounts to solve two Poisson problems as (169) in order to built $\chi$, to solve the interface equation to obtain $\lambda = v|_\Gamma$, then to solve two problems like (170) in order to obtain $v_i$.

When the differential multidomain problem (162) is approximated by spectral methods with a generalized Galerkin approach (or any other discretization method), the Steklov-Poincaré equation (173) has a finite dimensional counterpart and it takes the algebraic form $A\mathbf{u} = \mathbf{f}$, or equivalently:

$$\begin{bmatrix} A_{11} & 0 & A_{1\Gamma} \\ 0 & A_{22} & A_{2\Gamma} \\ A_{\Gamma 1} & A_{\Gamma 2} & A_{\Gamma\Gamma} \end{bmatrix} \begin{bmatrix} u_1 \\ u_2 \\ u_\Gamma \end{bmatrix} = \begin{bmatrix} f_1 \\ f_2 \\ f_\Gamma \end{bmatrix}. \tag{176}$$

$u_1$ (resp. $u_2$) is the vector of unknowns at the collocation nodes of $\overline{\Omega}_1\backslash\Gamma$ (resp. $\overline{\Omega}_2\backslash\Gamma$), $u_\Gamma$ is the unknowns vector of the nodes of $\Gamma$. A block Gauss elimination on the matrix $A$ gives:

$$\tilde{S}u_\Gamma = \tilde{f}_\Gamma \tag{177}$$

with

$$\tilde{S} \equiv (A_{\Gamma\Gamma} - A_{\Gamma 1}A_{11}^{-1}A_{1\Gamma} - A_{\Gamma 2}A_{22}^{-1}A_{2\Gamma}) \tag{178}$$

and

$$\tilde{f}_\Gamma = f_\Gamma - A_{\Gamma 1}A_{11}^{-1}f_1 - A_{\Gamma 2}A_{22}^{-1}f_2. \tag{179}$$

The matrix $\tilde{S}$ is referred to as the Schur complement of $A_{\Gamma\Gamma}$ in $A$ and the equation (177) is a discrete approximation of the interface equation (173).

The matrix $\tilde{S}$ is never explicitly assembled, but it is common practice to solve the system (177) by preconditioned iterative procedures where each matrix-vector product with $\tilde{S}$ involves two (in general $M$) subdomain solvers. The iterative procedures for solving equation (173) are traditionally referred to as *iterative substructuring methods*, since they introduce a sequence of differential subproblems in $\Omega_i$, for which the transmission conditions of (162) provide Dirichlet or Neumann data

at the internal boundary $\Gamma$.
We note that the Steklov-Poincaré operator $\mathcal{S}$ can be split in $\mathcal{S} = \mathcal{S}_1 + \mathcal{S}_2$ with $\mathcal{S}_i\lambda = \partial\mathcal{H}_i(\lambda)/\partial\mathbf{n}_i$ and, if we consider the Richardson method with preconditioner $\mathcal{P} = \mathcal{S}_1$ we obtain the so called Dirichlet-Neumann scheme ([8], [54], [11]). Otherwise the so-called Neumann-Neumann scheme ([9]) amounts to solve (173) by the preconditioned conjugate gradient with $\mathcal{P} = (\alpha\mathcal{S}_1^{-1} + (1-\alpha)\mathcal{S}_2^{-1})^{-1}$, $0 < \alpha < 1$.

The *Dirichlet Neumann scheme* was considered, e.g. by Bjorstad and Widlund ([8]), Bramble, Pasciak and Schatz ([11]) and Marini and Quarteroni ([54]) in the framework of finite element method and by Funaro, Quarteroni and Zanolli ([31]) for spectral methods. It reads as follows: given $\lambda^{(0)}$, $\forall k \geq 0$ solve:

$$\begin{cases} -\Delta u_1^{(k+1)} = f & \text{in } \Omega_1 \\ u_1^{(k+1)} = 0 & \text{on } \partial\Omega_1 \cap \partial\Omega \\ u_1^{(k+1)} = \lambda^{(k)} & \text{on } \Gamma, \end{cases} \tag{180}$$

$$\begin{cases} -\Delta u_2^{(k+1)} = f & \text{in } \Omega_2 \\ u_2^{(k+1)} = 0 & \text{on } \partial\Omega_2 \cap \partial\Omega \\ \dfrac{\partial u_2^{(k+1)}}{\partial \mathbf{n}_2} = -\dfrac{\partial u_1^{(k+1)}}{\partial \mathbf{n}_1} & \text{on } \Gamma, \end{cases} \tag{181}$$

then set $\lambda^{(k+1)} = \theta u_2^{(k+1)}|_\Gamma + (1-\theta)\lambda^{(k)}$, $\theta$ being a positive acceleration parameter in $(0,1)$ that can be computed dynamically ([54], [68]). The method can be generalized to more complex decompositions, with $M > 2$; in this case the subdomains are divided in two sets as in a chess-board; all the domains of the first set are treated as $\Omega_1$, the others as $\Omega_2$.
If a domain decomposition without internal cross-points is considered (a cross point is a subdomain vertex which is common to almost four subdomains) and the parameter $\theta$ is computed in the optimal way by the minimal contraction constant approach ([54], [68]), the condition number of the preconditioned system is independent of the polynomial degree $N$ of the spectral approximation but it linearly depends on the number of subdomains $M$. If we set $H = \max_i meas(\Omega_i)$ then there exists $C > 0$ independent of $N$ and $H$ such that

$$\chi(P^{-1}\tilde{S}) \leq CH^{-1} \tag{182}$$

where $P$ is the matrix associated to $\mathcal{P}$. Otherwise, in presence of internal cross points, we have

$$\chi(P^{-1}\tilde{S}) \leq CH^{-2}(1 + \log^2(HN^2)) \tag{183}$$

in accordance with ([68], [69]) and the numerical results in [33] (Fig. 2).

The *Neumann-Neumann scheme* was considered by Bourgat, Glowinski, Le Tallec and Vidrascu ([9]) and reads: given $\lambda^{(0)}$, $\forall k \geq 0$ solve:

$$\begin{cases} -\Delta u_i^{(k+1)} = f & \text{in } \Omega_i \\ u_i^{(k+1)} = 0 & \text{on } \partial\Omega_i \cap \partial\Omega \\ u_i^{(k+1)} = \lambda^{(k)} & \text{on } \Gamma, \end{cases} \qquad i = 1, 2, \tag{184}$$

$$\begin{cases} -\Delta v_i^{(k+1)} = f & \text{in } \Omega_i \\ v_i^{(k+1)} = 0 & \text{on } \partial\Omega_i \cap \partial\Omega \\ \dfrac{\partial v_i^{(k+1)}}{\partial \mathbf{n}_i} = \dfrac{\partial u_1^{(k+1)}}{\partial \mathbf{n}_1} + \dfrac{\partial u_2^{(k+1)}}{\partial \mathbf{n}_2} & \text{on } \Gamma, \end{cases} \qquad i = 1, 2, \tag{185}$$

then set $\lambda^{(k+1)} = \lambda^{(k)} - \theta(\sigma_1 v_1^{(k+1)}|_\Gamma - \sigma_2 v_2^{(k+1)}|_\Gamma)$, $\theta$ being a positive acceleration parameter in $(0,1)$ and $\sigma_1,\ \sigma_2$ two positive averaging coefficients.

Also for the Neumann-Neumann scheme a behaviour like (183) holds. Note that the computational cost of each iteration of the Neumann-Neumann method is double with respect to the computational cost of one iteration of the Dirichlet-Neumann scheme. Nevertheless this is balanced by the fact that the Neumann-Neumann scheme is twice faster than the Dirichlet-Neumann scheme in terms of number of iterations to converge with a given accuracy.

Another iterative substructuring approach is the *Robin method* proposed by Agoshkov and Lebedev ([1]) and analysed by P.L. Lions ([48]). It reads: given $u_2^{(0)}$, $\forall k \geq 0$ solve:

$$\begin{cases} -\Delta u_i^{(k+1)} = f & \text{in } \Omega_i \\ u_i^{(k+1)} = 0 & \text{on } \partial\Omega_i \cap \partial\Omega \qquad i = 1, 2 \\ \dfrac{\partial u_i^{(k+1)}}{\partial \mathbf{n}_i} + \theta u_i^{(k+1)} = -\dfrac{\partial u_j^{(k)}}{\partial \mathbf{n}_j} + \theta u_j^{(k)} & \text{on } \partial\Omega_i \cap \partial\Omega_j, \qquad j \neq i, \end{cases} \tag{186}$$

where $\theta$, is a non-negative acceleration parameter.

The Dirichlet-Neumann and the Robin methods are particular cases of the Lebedev-Agoshkov method ([46]) that reads: given $u_2^{(0)}$, $\forall k \geq 0$ solve:

$$\begin{cases} -\Delta u_1^{(k+1/2)} = f & \text{in } \Omega_1 \\ u_1^{(k+1/2)} = 0 & \text{on } \partial\Omega_1 \cap \partial\Omega \\ \dfrac{\partial u_1^{(k+1/2)}}{\partial \mathbf{n}_1} + p_k u_1^{(k+1/2)} = -\dfrac{\partial u_2^{(k)}}{\partial \mathbf{n}_2} + p_k u_2^{(k)} & \text{on } \partial\Omega_1 \cap \Gamma \end{cases} \tag{187}$$

then set

$$u_1^{(k+1)} = u_1^{(k)} + \alpha_{k+1}(u_1^{(k+1/2)} - u_1^{(k)}) \qquad \text{in } \overline{\Omega}_1; \tag{188}$$

solve:

$$\begin{cases} -\Delta u_2^{(k+1/2)} = f & \text{in } \Omega_2 \\ u_2^{(k+1/2)} = 0 & \text{on } \partial\Omega_2 \cap \partial\Omega \\ -q_k \dfrac{\partial u_2^{(k+1/2)}}{\partial \mathbf{n}_2} + u_2^{(k+1/2)} = -q_k \dfrac{\partial u_1^{(k+1)}}{\partial \mathbf{n}_1} + u_1^{(k+1)} & \text{on } \partial\Omega_2 \cap \Gamma \end{cases} \tag{189}$$

then set

$$u_2^{(k+1)} = u_2^{(k)} + \beta_{k+1}(u_2^{(k+1/2)} - u_2^{(k)}) \qquad \text{in } \overline{\Omega}_2 \tag{190}$$

with $p_k \geq 0$, $q_k \geq 0$, $\alpha_{k+1}, \beta_{k+1} \in \mathbb{R}$.
For $p_k = q_k = 0$ and $\alpha_k = \beta_k = 1$ we obtain the Dirichlet-Neumann scheme (180)-(181) where the role of $\Omega_1$ and $\Omega_2$ are reversed; for $p_k = \theta$, $q_k = 1/\theta$ and $\alpha_k = \beta_k = 1$ we obtain the Robin method (186).

Another approach to solve the Poisson problem via domain decomposition is the so-called Projection Decomposition Method (PDM) ([58], [33]). The main idea of this method consists of solving the interface equation (173) by the Galerkin projection method. The use of a piecewise-polynomial well-conditioned basis (in the sense of Mikhlin [55]) leads to a well-conditioned linear system for the coordinates of the Galerkin approximation in this basis, which can be solved effectively by the Conjugate Gradient method with the convergence rate independent of the system dimension. The combination of the piecewise-polynomials Galerkin approximation on the interface and the spectral collocation method in the subdomains results in high accuracy of the numerical solutions.
For the details on the construction of the well-conditioned basis we refer to ([58], [33]), here we briefly summarise the algorithm induced by the PDM:

- solve by spectral methods $M$ Poisson problems as (169) to obtain $u_0$ and compute the right hand side of the interface equation (written in weak form) with respect to the well-conditioned basis;
- solve by conjugate gradient the interface equation: at each conjugate gradient iteration we have to apply the discrete counterpart of the Steklov-Poincaré operator to a vector, that amounts to solve $M$ Poisson problems by spectral methods;
- solve by spectral methods $M$ Poisson problems as (170) to obtain $v$.

We note that at each step of this procedure the Poisson problems on the subdomains $\Omega_i$ are independent, thus this algorithm can be easily parallelised. The numerical results in [33] show that the rate of convergence of PDM depends on $H$ and $N$ as for the Dirichlet Neumann scheme (see 183) with a constant $C$ which is about 1/10 of the Dirichlet Neumann constant.

A way to improve the performance of domain decomposition methods, in terms of convergence rate, consists of incorporating a mechanism for global coupling, such as through a coarse grid problem based on a coarse mesh inside the computational domain.
For example, the *Bramble, Pasciak and Schatz method* ([11]) consists of preconditioning the Schur complement system by a block Jacobi matrix plus a coarse refinement involving the vertices of the subdomains. The condition number becomes logarithmic in $H/h$ ($h$ is the finite element mesh size), i.e. $\exists C > 0$ independent of $H$ and $h$ such that

$$\chi(P^{-1}\tilde{S}) \leq C\left(1 + \log^2\left(\frac{H}{h}\right)\right). \tag{191}$$

The performance of domain decomposition methods can be improved again by introducing overlapping decompositions as in the *additive Schwarz method* with *coarse correction* ([22], [27]), or the *2D vertex space method* of Smith ([80], [81]). For both these schemes it has been proved that $\exists C > 0$ independent of $H$ and $h$, but possibly dependent on the overlap $\beta$ such that

$$\chi(P^{-1}\tilde{S}) \leq C(\beta)\left(1 + \log\left(\frac{H}{h}\right)\right). \tag{192}$$

The overlapping methods have been largely applied to finite element discretization, but seldom to spectral context for the intrinsic difficulty of this approaches to combine "little" overlapping (i.e. little extensions of the elements) with Gaussian quadrature formulas. As a matter of fact these formulas have a fixed distribution of nodes and the addition of other nodes to the existing Gaussian set, in general causes the loss of precision of the quadrature formula.

Pavarino ([63], [64]) has proposed an overlapping additive Schwarz method for $p-$type finite elements. This idea amounts to consider quadrilateral finite elements $\Omega_i$ (of size $H$ and with high polynomial degree $p$), and to define the extended elements $\Omega'_k$ as the union of four elements $\Omega_{k1}, ...., \Omega_{k4}$ which have a common vertex (see Fig. 6). The elements $\Omega'_k$ are defined for each vertex internal to the computational domain $\Omega$ and they form an overlapping decomposition with an overlap of the same size of the original elements ($H$). Then an additive Schwarz method is considered to solve the multidomain problem with a coarse refinement involving the vertex of the original decomposition. The rate of convergence of this domain decomposition

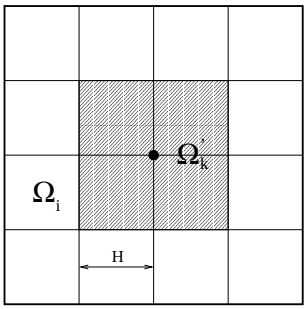


Figure 6: The original elements $\Omega_i$ and the extended elements of the overlapped decomposition $\Omega'_k$ used by Pavarino.

solver is independent of both the size $H$ of the elements and the polynomial degree $p$ ([63]).

**Remark 4.1** We have seen in Sec. 1 that when a differential problem is approximated by spectral methods, an optimal preconditioner is the matrix obtained by the bilinear finite element approximation of the same problem on the Legendre Gauss-Lobatto grid. This preconditioner can be also used inside a multidomain approach. The system (162), approximated by spectral methods, can be faced by a preconditioned iterative method (e.g. the Richardson or conjugate gradient method) where the preconditioner is referred to the global grid of collocation nodes, i.e. the union of the Legendre Gauss-Lobatto nodes of all the subdomains $\Omega_i$ ($i = 1, ..., M$) (see [18], [26], [73]). Each step of the iterative solver consists of evaluating the residual of the spectral multidomain system and then solving a finite element problem in the global domain. The method converges with a rate that is substantially independent of the number of gridpoints ([73], [82]).□

Another way to use the bilinear finite element preconditioner consists of building the inexact additive Schwarz preconditioner as described in Sec. 1.5 for the spectral element method.

### 4.2 The Stokes problem

Consider now the generalized Stokes system (114), and the notations introduced in the previous subsection. The multidomain form of the Stokes system reads: for $i = 1, ..., M$ find $(\mathbf{u}_i, p_i)$ such that:

$$\begin{cases} \alpha \mathbf{u}_i - \nu \Delta \mathbf{u}_i + \nabla p_i = \mathbf{f} & \text{in } \Omega_i \\ \mathbf{u}_i = \mathbf{u}_j & \text{on } \Gamma_{ij} = \partial\Omega_i \cap \partial\Omega_j \\ \nu \dfrac{\partial \mathbf{u}_i}{\partial \mathbf{n}_i} - p_i \mathbf{n}_i = -\nu \dfrac{\partial \mathbf{u}_j}{\partial \mathbf{n}_j} - p_j \mathbf{n}_j & \text{on } \Gamma_{ij} \\ \mathbf{u}_i = \mathbf{0} & \text{on } \partial\Omega_i \cap \partial\Omega \\ \nabla \cdot \mathbf{u}_i = 0 & \text{in } \Omega_i. \end{cases} \tag{193}$$

The transmission conditions on $\Gamma_{ij}$ enforce the continuity of the solution and of the normal component of the stress tensor.
As for the Poisson problem, one can prove the equivalence between the systems (114) and (193) and introduce the Steklov-Poincaré operator, the interface equation and the iterative methods based on transmission conditions.

We take into account the variational form (116)-(117) of (114); the variational multidomain form of (193) with $M = 2$ reads:
find $(\mathbf{u}_1, p_1) \in \mathbf{V}_1 \times L^2(\Omega_1)$, $(\mathbf{u}_2, p_2) \in \mathbf{V}_2 \times L^2(\Omega_2)$:

$$\begin{cases} a_1(\mathbf{u}_1, \mathbf{v}_1) + b_1(\mathbf{v}_1, p_1) = (\mathbf{f}, \mathbf{v}_1)_{L^2(\Omega_1)} & \forall \mathbf{v}_1 \in [V_1^0]^2 \\ b_1(\mathbf{u}_1, q_1) = 0 & \forall q_1 \in L^2(\Omega_1) \\ \mathbf{u}_1 = \mathbf{v}_1 & \text{on } \Gamma \\ a_2(\mathbf{u}_2, \mathbf{v}_2) + b_2(\mathbf{v}_2, p_2) = (\mathbf{f}, \mathbf{v}_2)_{L^2(\Omega_2)} & \forall \mathbf{v}_2 \in [V_2^0]^2 \\ b_2(\mathbf{u}_2, q_2) = 0 & \forall q_2 \in L^2(\Omega_2) \\ a_2(\mathbf{u}_2, E_2\mu) + b_2(E_2\mu, p_2) = (\mathbf{f}, E_2\mu)_{L^2(\Omega_2)} & \\ \quad +(\mathbf{f}, E_1\mu)_{L^2(\Omega_1)} - a_1(\mathbf{u}_1, E_1\mu) - b_1(E_1\mu, p_1) & \forall \mu \in [\Lambda]^2 \\ \displaystyle\int_{\Omega_1} p_1 \mathrm{d}\Omega_1 + \int_{\Omega_2} p_2 \mathrm{d}\Omega_2 = 0 & \end{cases} \tag{194}$$

where $\forall \mathbf{w}_i,\ \mathbf{v}_i \in [V_i]^2,\ \forall q_i \in L^2(\Omega_i)$:

$$a_i(\mathbf{w}_i, \mathbf{v}_i) = \int_{\Omega_i} \frac{\nu}{2} \sum_{j,l=1}^{2} \left( \frac{\partial (\mathbf{w}_i)_l}{\partial x_j} + \frac{\partial (\mathbf{w}_i)_j}{\partial x_l} \right) \left( \frac{\partial (\mathbf{v}_i)_l}{\partial x_j} + \frac{\partial (\mathbf{v}_i)_j}{\partial x_l} \right), \tag{195}$$

$$b_i(\mathbf{w}_i, q_i) = -\int_{\Omega_i} (\nabla \cdot \mathbf{w}_i) q_i \mathrm{d}\Omega_i, \tag{196}$$

and $E_i : [\Lambda]^2 \to [V_i]^2$ is a Stokes extension operator.

To construct the interface equation for the Stokes problem, we write $\mathbf{u} = \mathbf{u}_0 + \mathbf{v}$ and $p = p_0 + \pi$, where $(\mathbf{u}_0, p_0)$ is the solution of

$$\begin{cases} \alpha \mathbf{u}_{0,i} - \nu \Delta \mathbf{u}_{0,i} + \nabla p_{0,i} = \mathbf{f} & \text{in } \Omega_i \\ \nabla \cdot \mathbf{u}_{0,i} = 0 & \text{in } \Omega_i \\ \mathbf{u}_{0,i} = \mathbf{0} & \text{on } \partial\Omega_i \end{cases} \qquad i = 1, 2 \tag{197}$$

(as usual $\mathbf{u}_{0,i} = \mathbf{u}_0|_{\Omega_i}$, $p_{0,i} = p_0|_{\Omega_i}$), while $(\mathbf{v}, \pi)$ is the solution of

$$\begin{cases} \alpha \mathbf{v}_i - \nu \Delta \mathbf{v}_i + \nabla \pi_i = \mathbf{0} & \text{in } \Omega_i \\ \nabla \cdot \mathbf{v}_i = 0 & \text{in } \Omega_i \\ \mathbf{v}_i = \mathbf{0} & \text{on } \partial\Omega_i \cap \partial\Omega \\ \mathbf{v}_i = \boldsymbol{\lambda} & \text{on } \partial\Omega_i \cap \Gamma \end{cases} \qquad i = 1, 2 \tag{198}$$

(with $\mathbf{v}_i = \mathbf{v}|_{\Omega_i}$, $\pi_i = \pi|_{\Omega_i}$).

In order to achieve the equivalence with problem (193), $\boldsymbol{\lambda}$ has to be chosen in a way that the following interface equation be satisfied:

$$\nu \frac{\partial \mathbf{u}_1}{\partial \mathbf{n}_1} - p_1 \mathbf{n}_1 = -\nu \frac{\partial \mathbf{u}_2}{\partial \mathbf{n}_2} - p_2 \mathbf{n}_2 \qquad \text{on } \Gamma. \tag{199}$$

This can be equivalently written as:

$$\mathcal{S}_S \boldsymbol{\lambda} = \boldsymbol{\chi}_S \tag{200}$$

with

$$\boldsymbol{\chi}_S = -\left( \nu \frac{\partial \mathbf{u}_{0,1}}{\partial \mathbf{n}_1} - p_1 \mathbf{n}_1 + \nu \frac{\partial \mathbf{u}_{0,2}}{\partial \mathbf{n}_2} - p_2 \mathbf{n}_2 \right) \tag{201}$$

and

$$\mathcal{S}_S \boldsymbol{\lambda} = \mathcal{S}_S^1 \boldsymbol{\lambda} + \mathcal{S}_S^2 \boldsymbol{\lambda} = \left( \nu \frac{\partial \mathbf{v}_1}{\partial \mathbf{n}_1} - \pi_1 \mathbf{n}_1 \right) + \left( \nu \frac{\partial \mathbf{v}_2}{\partial \mathbf{n}_2} - \pi_2 \mathbf{n}_2 \right). \tag{202}$$

Equation (200) is the interface equation for the generalized Stokes problem and $\mathcal{S}_S$ is the associate Steklov-Poincaré operator. To solve the interface equation (200) amounts to solve again two generalized Stokes problems on $\Omega_i$ in order to find $(\mathbf{u}_0, p_0)$ and compute $\boldsymbol{\chi}_S$. Then, solve the equation on $\boldsymbol{\lambda}$ and, finally, solve two generalized Stokes problems on $\Omega_i$ in order to find $(\mathbf{v}, \pi)$.
As for the Poisson problem we can formulate the finite dimensional counterpart of (200) and obtain the Schur complement matrix.

Some iterative procedure to solve the discrete interface equation on non-overlapping decompositions are the Dirichlet-Neumann scheme ([67], [54], [70], [11]) and the Neumann-Neumann scheme ([9]).

The Dirichlet-Neumann method for the generalized Stokes system on the two-domain decomposition reads: given $\boldsymbol{\lambda}^{(0)}$, $\forall k \geq 0$ solve:

$$\begin{cases} \alpha \mathbf{u}_1^{(k+1)} - \Delta \mathbf{u}_1^{(k+1)} + \nabla p_1^{(k+1)} = \mathbf{f} & \text{in } \Omega_1 \\ \nabla \cdot \mathbf{u}_1 = 0 & \text{in } \Omega_1 \\ \mathbf{u}_1^{(k+1)} = \mathbf{0} & \text{on } \partial\Omega_1 \cap \partial\Omega \\ \mathbf{u}_1^{(k+1)} = \boldsymbol{\lambda}^{(k)} & \text{on } \Gamma \cap \partial\Omega_1, \end{cases} \tag{203}$$

$$\begin{cases} \alpha \mathbf{u}_2^{(k+1)} - \Delta \mathbf{u}_2^{(k+1)} + \nabla p_2^{(k+1)} = \mathbf{f} & \text{in } \Omega_2 \\ \nabla \cdot \mathbf{u}_2 = 0 & \text{in } \Omega_2 \\ \mathbf{u}_2^{(k+1)} = \mathbf{0} & \text{on } \partial\Omega_2 \cap \partial\Omega \\ \nu \dfrac{\partial \mathbf{u}_2^{(k+1)}}{\partial \mathbf{n}_1} - p_2^{(k+1)} \mathbf{n}_2 = -\nu \dfrac{\partial \mathbf{u}_1^{(k+1)}}{\partial \mathbf{n}_1} - p_1^{(k+1)} \mathbf{n}_1 & \text{on } \Gamma \cap \partial\Omega_2, \end{cases} \tag{204}$$

then set $\boldsymbol{\lambda}^{(k+1)} = \theta \mathbf{u}_2^{(k+1)}|_\Gamma + (1-\theta)\boldsymbol{\lambda}^{(k)}$, $\theta$ being a positive acceleration parameter in $(0,1)$.
The initial datum $\boldsymbol{\lambda}^{(0)}$ has to satisfy a compatibility condition with respect to the continuity equation $\nabla \cdot \mathbf{u} = 0$. As a consequence of the divergence theorem, for any $\Omega_k \subset \Omega$, it holds

$$\int_{\Omega_k} \nabla \cdot \mathbf{u} = \int_{\partial\Omega_k} \mathbf{u} \cdot \mathbf{n}_k = 0 \tag{205}$$

and, under the assumption that $\mathbf{u}|_{\partial\Omega} = \mathbf{0}$, we have

$$\int_\Gamma \mathbf{u} \cdot \mathbf{n}_k = -\int_{\partial\Omega_k \setminus \Gamma} \mathbf{u} \cdot \mathbf{n}_k = 0. \tag{206}$$

It follows that $\boldsymbol{\lambda}^{(0)}$ must satisfy the condition

$$\int_\Gamma \boldsymbol{\lambda}^{(0)} \cdot \mathbf{n}_1 = 0, \tag{207}$$

which guarantees that

$$\int_\Gamma \boldsymbol{\lambda}^{(k)} \cdot \mathbf{n}_1 = 0, \qquad \forall k \geq 1. \tag{208}$$

(See [72]).

The Dirichlet-Neumann method converges with a rate independent of $N$, provided that the inf-sup condition (121) is satisfied with a constant $\beta$ uniformly bounded from below ([67]). It can also be used as an iterative substructuring procedure to solve the global system arising from a spectral element approximation of the Stokes equations.

Projection Decomposition Method can be considered to solve the interface equation (200) (see [59]). As for the Poisson problem, a well-conditioned basis is constructed to approximate the equation on the interface $\Gamma$ by the projection Galerkin method. Its rate of convergence is independent of the number of basis functions on the interface as well as the polynomial degree which is used inside each subdomain.

## 4.3 The Navier-Stokes equations

A multidomain formulation of Navier-Stokes equations can be based on the stabilized SEM. Using the notations of Sec. 1.5 and a decomposition of $\Omega$ like (97), a system similar to (138) is obtained. However, now the discrete solution $[\mathbf{u}_\mathcal{H}, p_\mathcal{H}]$ is sought in $\mathbf{V}_\mathcal{H} \times Q_\mathcal{H}$, with

$$\mathbf{V}_\mathcal{H} = [V_\mathcal{H} \cap H_0^1(\Omega)]^2, \qquad Q_\mathcal{H} = V_\mathcal{H} \cap L_0^2(\Omega), \tag{209}$$

and any discrete inner product $(\cdot,\cdot)_{N,\Omega}$ is replaced with its spectral element counterpart. Also the stabilization parameters ar referred to the spectral element discretization, in particular $T_k$ plays the role of $\Omega$ in (141)-(142).

At each time level the matrix of the system is sparse and its condition number depends heavily on the parameters of the spectral element discretization, say the mesh size $H$ and the polynomial degree $N$ on each element. Numerical results (see [34]) show that the condition number of the matrix $A_{\mathcal{H}}$, arising from the stabilized spectral element approximation, is

$$\chi(A_{\mathcal{H}}) \leq CN^6H^{-4}, \tag{210}$$

for a suitable constant $C$ independent of $N$ and $H$. Then it is mandatory to solve the system by a preconditioned iterative method. Instead of a global preconditioner, that requires many storage locations to be stored and incompletely factorized, an element by element bilinear preconditioner based on the same stabilized approach used for the primary problem can be used.

We denote by $A_k$ the square matrix of dimension $3(N+1)^2$ which is the block matrix associated to the stabilized spectral element approximation of Navier Stokes problem on the element $T_k \in \mathcal{T}_H$. Besides, $\mathbf{R}_k^T$ is a rectangular matrix of dimensions $3N_h^2 \times 3(N+1)^2$, ($N_h$ is the total number of nodes in the computational domain $\Omega$) which is the extension matrix associated to $T_k$ (see Sec. 1.5). Then

$$A_{\mathcal{H}} = \sum_{k=1}^{Ne} \mathbf{R}_k^T A_k \mathbf{R}_k. \tag{211}$$

Now we denote by $A_k^{fe}$ the block matrix associated to the stabilized bilinear spectral element matrix on $T_k$ (it has the same dimensions of $A_k$) and we define a block Jacobi preconditioner as follows:

$$P^{-1} = \sum_{k=1}^{Ne} \mathbf{R}_k^T (A_k^{fe})^{-1} \mathbf{R}_k. \tag{212}$$

Numerical results on a decomposition of $\Omega$ in $Ne = M_1 \times M_1$ elements of size $H$ ([32]) show that

$$\chi(P^{-1}A_{\mathcal{H}}) \leq CN^2H^{-2}. \tag{213}$$

Even if this preconditioner is non optimal, the numerical results point out substantial reduction of the iteration number with respect to an unpreconditioned system, but also to a diagonally preconditioned system. All results presented in the following section are obtained using the BiCGStab iterative method ([24]) with the preconditioner (212).

# 5 Numerical results

We present here some numerical results obtained by the approximation of incompressible Navier-Stokes equations (113) with the stabilized spectral element method. Different test cases are addressed.

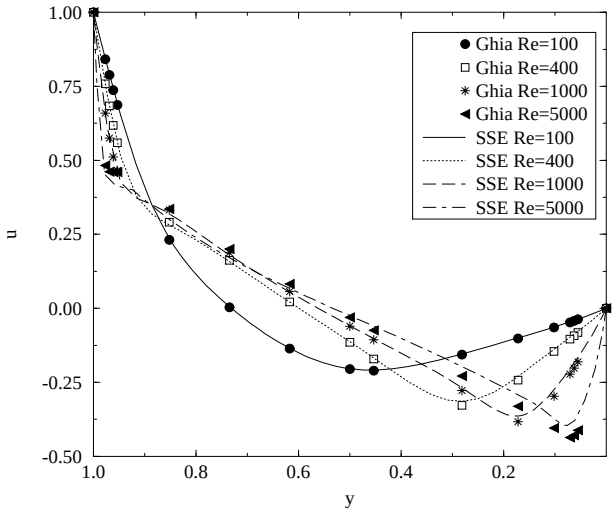


Figure 7: Profiles of $u$ velocities along vertical lines through geometric center of the cavity.

### 5.1 Driven cavity flow

This test case shows the motion of a flow inside a plane square domain $\Omega = (0,1)^2$ with tangential velocity prescribed on the top boundary $\mathbf{u}_\infty = (1,0)^T$. We define the Reynolds number as $Re = D\|\mathbf{u}_\infty\|/\nu$ where $D$ is the measure of the side of $\Omega$ and $\mathbf{u}_\infty$ is the prescribed tangential velocity on the top side. On the vertical sides and on the bottom horizontal side a no-slip boundary condition is imposed.

The problem has been solved by the stabilized spectral elements (SSE), and by the Euler semi-implicit time advancing scheme (134).

We compare our results with those of Ghia et al. ([35]) about the profiles of the velocity components $u$ and $v$ along vertical and horizontal (respectively) lines through geometric center of the cavity (see figures 7 and 8). The solid lines represent the numerical solution obtained by SSE at different Reynolds numbers, while the symbols represent the numerical data reported in Tables I and II in [35].

In Tab. 3 we compare the space discretization used in [35] and by SSE. $N$ and $M$ stand for the polynomial degree in each spectral element (in each direction) and the number of elements in each direction respectively. Unless otherwise specified the decomposition of $\Omega$ is uniform.

In figures 9 and 10 we report the streamline contours for the cavity flow configurations, that we have obtained for $Re$=400, 1000, 5000, 10000. Finally in Fig. 11 we show the pressure for $Re$=5000 and $Re$=10000.

### 5.2 Creeping flow in a wedge

The computational domain $\Omega$ for this test case ([50]), and its spectral element partition are represented in figure 12. Inside each element, polynomials of degree $N = 6$ have been considered and the Euler semi-implicit scheme with $\Delta t = .01$ has been

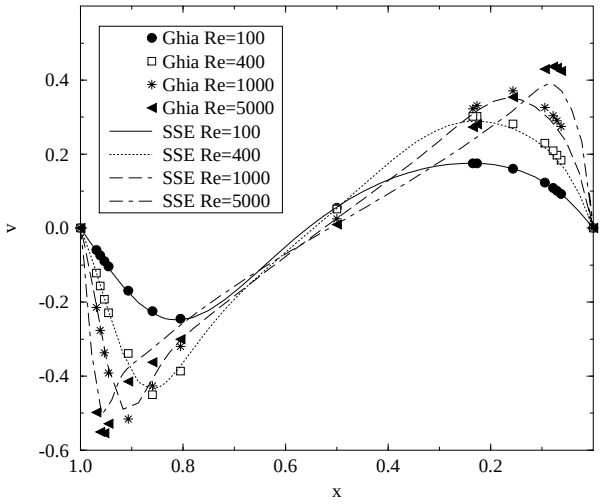


Figure 8: Profiles of $v$ velocities along horizontal lines through geometric center of the cavity.

| $Re$ | 100 | 400 | 1000 | 5000 | 10000 |
|---|---|---|---|---|---|
| Ghia | $129 \times 129$ | $129 \times 129$ | $129 \times 129$ | $257 \times 257$ | $257 \times 257$ |
| discretization | 16641 | 16641 | 16641 | 66049 | 66049 |
| SSE | $N = 8$ | $N = 8$ | $N = 6$ | $N = 6$ | $N = 6$ |
| discretization | $M = 6$ | $M = 6$ | $M = 10$ | $M = 12$ | $M = 12$ |
| | (2401) | (2401) | (3721) | (5329) | (5329) |

Table 3: The number of nodes of the space discretization used in the "Driven Cavity" test case. $M$ denotes the number of elements in each space direction.

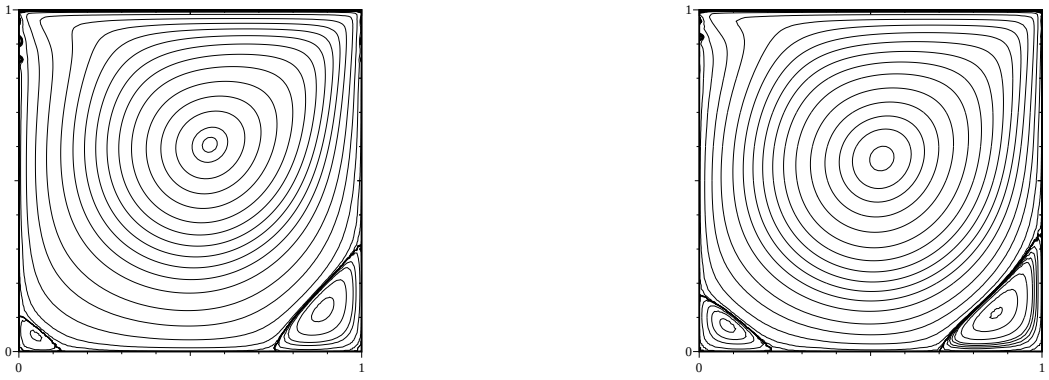


Figure 9: Streamlines for $Re$=400 (left) and $Re$=1000 (right).

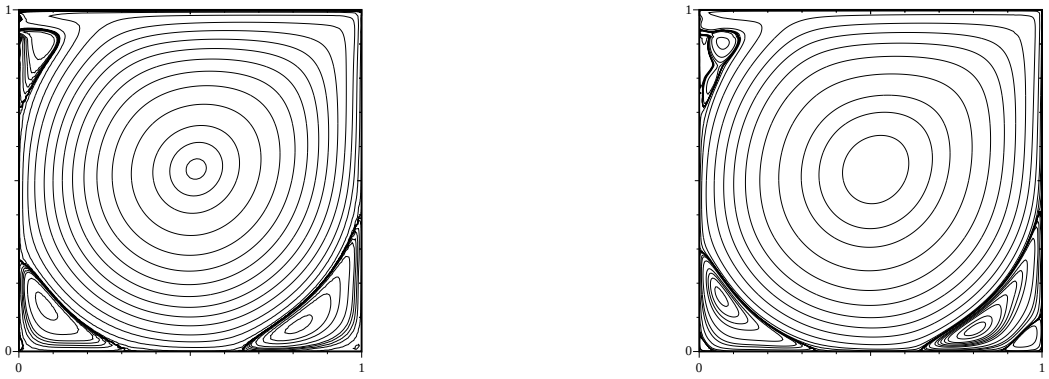


Figure 10: Streamlines for $Re$=5000 (left) and $Re$=10000 (right).

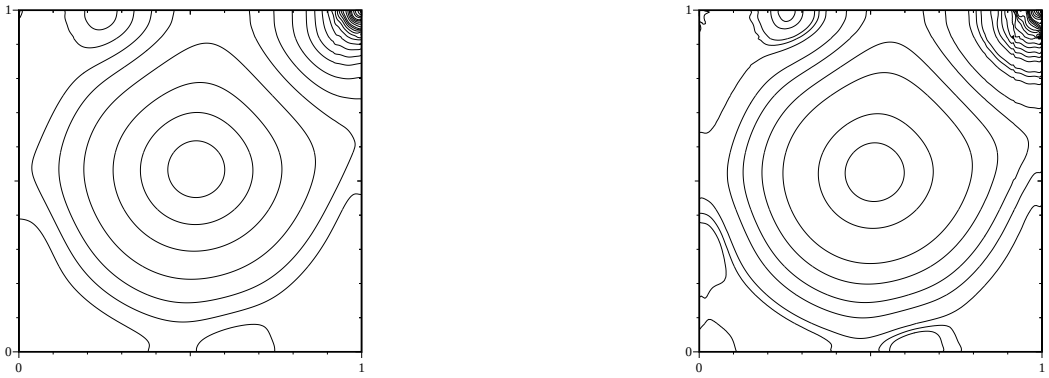


Figure 11: The pressure for $Re$=5000 (left) and $Re$=10000 (right).

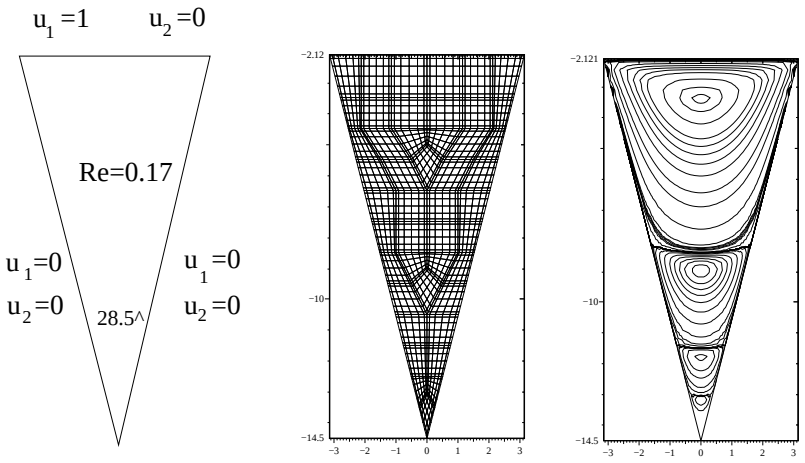


Figure 12: The geometry of the problem *creeping flow in a wedge* (left), the domain partition (center) and the stream-functions (right) relative to the *creeping flow in a wedge*.

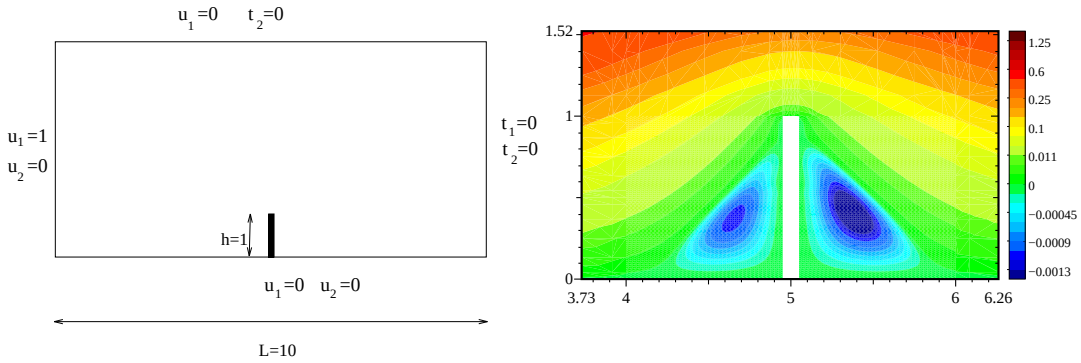


Figure 13: The geometry (left) and a zoom on the stream-function (right) relative to the test case: *Uniform flow past a fence*.

used. The motion is driven by steady motion of the fluid at the top of the edge; the Reynolds number is $Re = 0.17$ and it is based on the peripheral speed $\mathbf{u}_\infty = (1, 0)^T$, $\nu = 36.39$ and the top side length $D = 2\pi$. In figure 12 (right) the computed stream functions are shown.

### 5.3 Uniform flow past a fence

We consider the motion of a fluid in the domain $\Omega = (0, 10) \times (0, 5)$ in the presence of a fence of height $D = 1$ and width equal to 0.1. We set the inflow velocity $\mathbf{u}_\infty = (1, 0)^T$, a viscosity $\nu = 71.43$ so that $Re = 0.014$. The problem geometry and the boundary conditions used are shown in Fig. 13. The domain has been partitioned in 24 elements with polynomial degree $N = 6$ in each element. The computed stream functions are shown in Fig. 13.

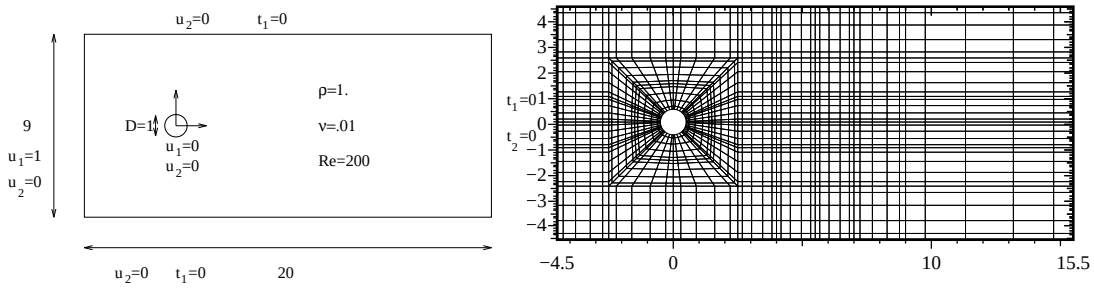


Figure 14: The geometry (left) and the partition of the computational domain (right) for the test case of *uniform flow past a circular cylinder.*

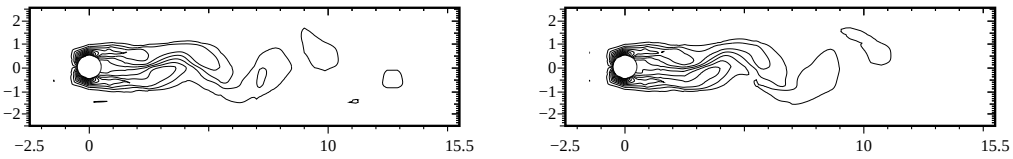


Figure 15: The vorticity at $t = 111$ (left) and $t = 112$(right).

## 5.4 Uniform flow past a circular cylinder

This unsteady problem represents the motion of a flow past a circular obstacle. The computational domain is $\Omega = (-4.5, 15.5) \times (-4.59, 4.5)$ and a circular obstacle, with diameter $D = 1$, is centered at $(0, 0)$. The lack of symmetry on the geometry has been adopted on purpose in order to generate periodic motion of the fluid (see [79]). This motion is known in the literature as *Von Karman vortex street.*

The computational domain has been discretized in 64 spectral elements with polynomial degree $N = 6$ in each direction. The total number of nodes is 1700. The boundary conditions are assigned as they can be observed in figure (14), where $t_1$ and $t_2$ represent the two components of the normal component of the stress tensor $\tilde{T}\mathbf{n} = -p\mathbf{n} + (\mathbf{n} \cdot \nabla)\mathbf{u}$. The semi-implicit Euler scheme has been used with $\Delta t = .05$. After an initially phase of transition, the motion becomes periodic in time with a period $T = 6$, corresponding to a Strouhal number $St = D/(\|\mathbf{u}_\infty\|T) = 0.167$.

In figure (14) the discretization of the computational domain is shown while in figures (15)-(17) we show the vorticity for $Re$=200 at six different time steps of a period.

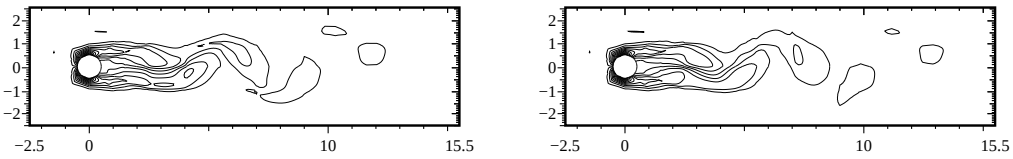


Figure 16: The vorticity at $t = 113$ (left) and $t = 114$(right).

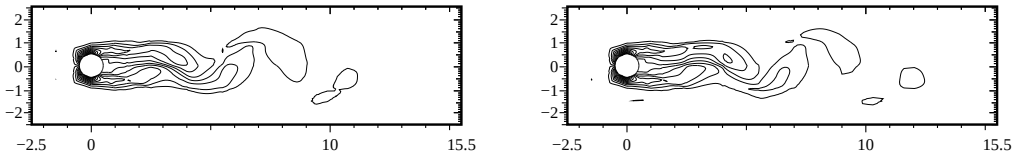


Figure 17: The vorticity at $t = 115$ (left) and $t = 116$ (right).

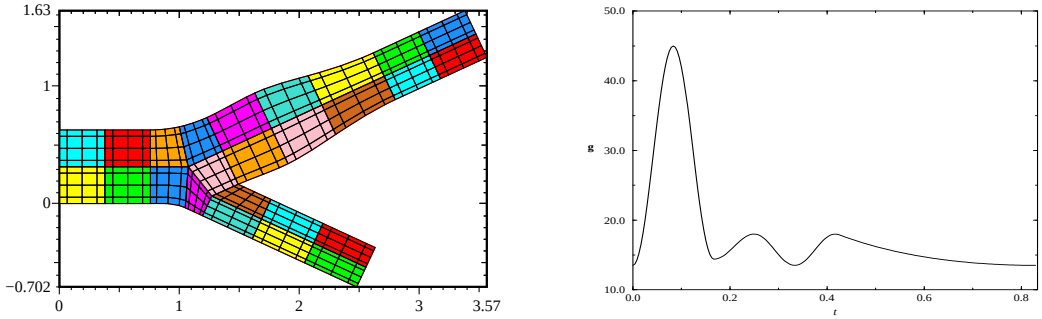


Figure 18: The spectral element mesh on the branching plane (left) and the time-dependent velocity profile $\mathbf{g}(x_2, t)$.

### 5.5 Two dimensional model of pulsatile Newtonian flow in the human carotid bifurcation

This model problem is considered in biomechanical literature as a simplification of the more complex 3-D problem.
The computational domain and its spectral elements decomposition are shown in Fig. 18. The basic shape of the model agrees with the model of Bharadvaj ([7]) and the geometry parameters are based upon the data described by Ku et al. ([65], [45]). Using the common carotid diameter $D = 0.62$cm as characteristic length and a reference blood viscosity $\nu = 0.035$, the maximum Reynolds number inside a period of the motion is $Re_{\max} \simeq 800$. The assumed pulse frequency is 80 strokes per minute.
At the inflow boundary (the left vertical side) a fully developed time-dependent velocity profile $\mathbf{g} = \mathbf{g}(x_2, t)$ is prescribed (according to [45], see Fig. 18); at the rigid walls the no slip condition $\mathbf{u} = \mathbf{0}$ is applied, while at the outflow boundary a no-friction condition is imposed (i.e. $\tilde{T}\mathbf{n} = -p\mathbf{n} + (\mathbf{n} \cdot \nabla)\mathbf{u} = \mathbf{0}$).

The discretization is based on 25 spectral elements with polynomial degree $N = 4$ and the global number of nodes is 461. The velocity field and the stream functions in the branching plane during the pulse cycle ($T = 0.8\overline{3}$) are shown in Figures 19-22, in accordance with the results of ([65]).

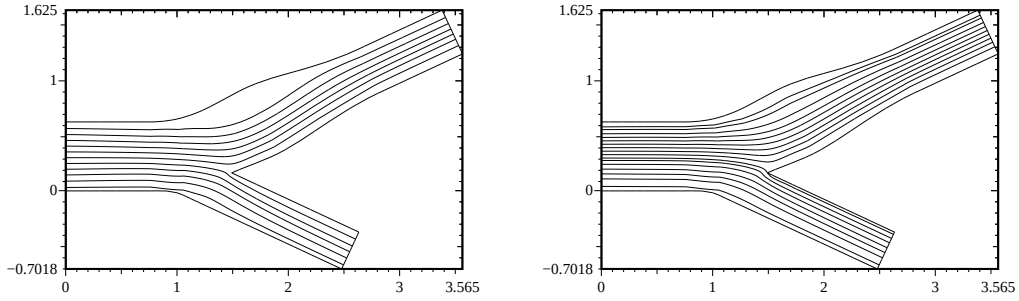


Figure 19: The velocity field and the stream functions in the branching plane during the pulse cycle at $t = 0.0$ (left) and $t = 0.05$ (right).

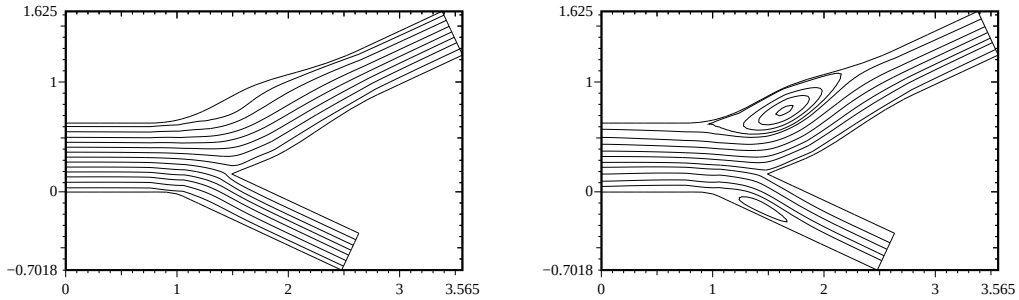


Figure 20: The velocity field and the stream functions in the branching plane during the pulse cycle at $t = 0.09$ (left) and $t = 0.14$ (right).

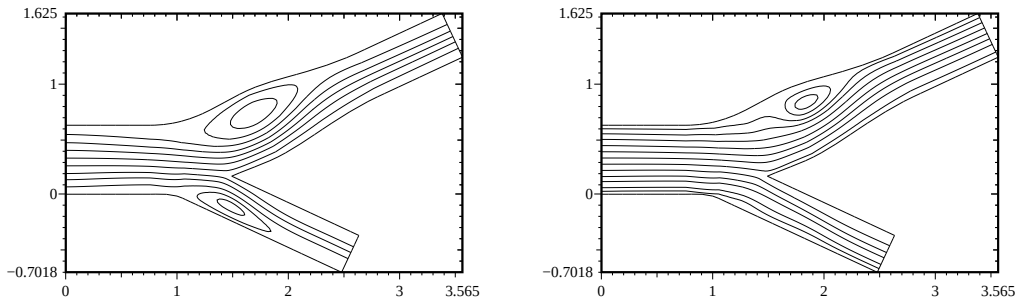


Figure 21: The velocity field and the stream functions in the branching plane during the pulse cycle at $t = 0.17$ (left) and $t = 0.26$ (right).

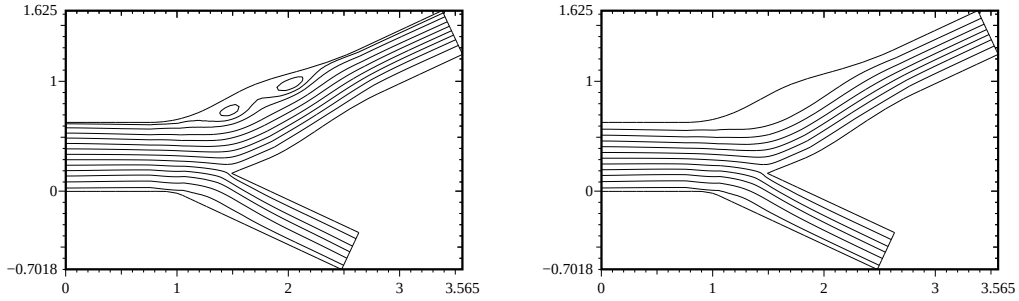


Figure 22: The velocity field and the stream functions in the branching plane during the pulse cycle at $t = 0.36$ (left) and $t = 0.8$ (right).

## References


[1] V.I. Agoshkov and V.I. Lebedev. The Poincaré-Steklov's operators and the domain decomposition algorithms in variational problems. *Computational Processes and Systems*, 2:173–227, 1985. NAUKA, Moscow, (in Russian).

[2] I. Babuška. The finite element method with Lagrangian multipliers. *Numer. Math.*, 20:179–192, 1973.

[3] I. Babuška and M.R. Dorr. Error estimates for the combined $h$ and $p$ versions of the finite element method. *Numer.Math.*, 37:257–277, 1981.

[4] I. Babuška and M. Suri. The $h - p$ version of the finite element method with quasi-uniform meshes. *Mathematical Modelling and Numerical Analysis*, 21:199–238, 1987.

[5] C. Bernardi and Y. Maday. *Approximations Spectrales de Problèmes aux Limites Elliptiques.* Springer Verlag, Paris, 1992.

[6] C. Bernardi, Y. Maday, and A.T. Patera. A new nonconforming approach to domain decomposition: the mortar element method. In H. Brezis and J.L. Lions, editors, *Nonlinear Partial Differential Equations and Their Applications.* Collège de France Seminar, 1989.

[7] B.K. Bharadvaj, R.F. Mabon, and D.P. Giddens. Steady flow in a model of the human carotid bifurcation. Part I- Flow visualisation. *J. Biomechanics*, 15:349–362, 1982.

[8] P. Bjorstad and O.B. Widlund. Iterative methods for the solution of elliptic problems on regions partitioned into substructures. *SIAM J. Numer. Anal.*, 23:1097–1120, 1986.

[9] J.F. Bourgat, R. Glowinski, P. Le Tallec, and M.Vidrascu. Variational formulation and algorithm for trace operator in domain decomposition calculations. In J.Perieaux T.F.Chan, R.Glowinski and O.B.Widlund, editors, *Domain Decomposition Methods for Partial Differential Equations*, Philadelphia, 1989. SIAM.

[10] J.P Boyd. *Chebyshev and Fourier Spectral Methods.* Springer-Verlag, Berlin, 1989.

[11] J. Bramble, J. Pasciak, and A. Schatz. An iterative method for elliptic problems on regions partitioned into substructures. *Math. Comp.*, 46:361–369, 1986.

[12] F. Brezzi. On the existence, uniqueness and approximation of saddle-point problems arising from Lagrange multipliers. *R.A.I.R.O Anal. Numér.*, 8 (R2):129–151, 1974.

[13] F. Brezzi and J. Pitkaranta. On the stabilization of finite element approximations of the Stokes equations. In *Efficient Solutions of Elliptic Systems, Note on Numerical Fluid Mechanics*, volume 10, pages 11–19. W. Hackbusch, 1984.

[14] A.N. Brooks and T.J.R. Hughes. Streamline Upwind/Petrov-Galerkin formulations for convection dominated flows with particular emphasis on the incompressible Navier-Stokes equations. *Comput. Meth. Appl. Mech. Engrg.*, 32:199–259, 1982.

[15] C. Canuto. Stabilization of spectral methods by finite element bubble functions. *Comput. Methods Appl. Mech. Engrg.*, 116:13–26, 1994.

[16] C. Canuto, M. Y. Hussaini, A. Quarteroni, and T. A. Zang. *Spectral Methods in Fluid Dynamics*. Springer Verlag, Berlin, 1988.

[17] C. Canuto and V. Van Kemenade. Bubble-stabilized spectral methods for the incompressible Navier-Stokes equations. *Comput. Methods Appl. Mech. Engrg.*, 135:35–61, 1996.

[18] C. Canuto and P. Pietra. Boundary and interface conditions within a finite element preconditioner for spectral methods. *J. Comput. Phys.*, 91:310–343, 1990.

[19] C. Canuto and A. Quarteroni. Approximation results for orthogonal polynomials in Sobolev spaces. *Math. Comput.*, 38:67–86, 1982.

[20] C. Canuto and A. Quarteroni. Preconditioned minimal residual methods for Chebyshev spectral calculations. *J. Comput. Phys.*, 60:315–337, 1985.

[21] M.A. Casarin. Quasi-optimal Schwarz methods for the conforming spectral element discretization. *SIAM J. Numer. Anal.*, 34(6):2482–2502, 1997.

[22] T.F. Chan and T.P. Mathew. Domain decomposition algorithms. In *Acta Numerica*, pages 61–143. Cambridge Univ. Press, 1994.

[23] J.W. Cooley and J.W. Tukey. An Algorithm for the Machine Calculation of Complex Fourier Series. *Math. Comput.*, 19:297–301, 1965.

[24] H.A. Van der Vorst. Bi-CGStab: A faster smoothly converging variant of Bi-CG for the solution of nonsymmetric linear systems. *SIAM J. Sci. Stat. Comput.*, 13(2):631–644, 1992.

[25] M.O. Deville and E.H. Mund. Chebyshev pseudospectral solution of second-order elliptic equations with finite element preconditioning. *J. Comput. Phys.*, 60:517–533, 1985.

[26] M.O. Deville and E.H. Mund. Finite element preconditioning for pseudospectral solutions of elliptic problems. *SIAM J. Sci. Stat. Comput.*, 11:311–342, 1990.

[27] M. Dryja and O. Widlund. Some domain decomposition algorithms for elliptic problems. In L.Hayes and D. Kincaid, editors, *Iterative methods for large linear systems*, pages 273–291. Academic, 1989.

[28] M. Dryja and O. Widlund. Additive Schwarz methods for elliptic finite element problems in three dimensions. In T.F.Chan, D.E. Keyes, G.A. Meurant, J.S. Scroggs, and R.G. Voigt, editors, *Fifth Conf. on Domain Decomposition Methods for Partial Differential Equations*, Philadelphia, 1992. SIAM.

[29] M. Dubiner. Spectral methods on triangles and other domains. *J. Sci. Comput.*, 4:345–390, 1991.

[30] L.P. Franca and S.L. Frey. Stabilized finite element methods: II. The Incompressible Navier-Stokes Equations. *Comput. Meth. Appl. Mech. Engrg.*, 99:209–233, 1992.

[31] D. Funaro, A. Quarteroni, and P. Zanolli. An iterative procedure with interface relaxation for domain decomposition methods. *SIAM J.Numer.Anal.*, 25:1213–1236, 1988.

[32] P. Gervasio. *Risoluzione di equazioni alle derivate parziali con metodi spettrali in regioni partizionate in sottodomini.* PhD thesis, Università degli Studi di Milano, 1995.

[33] P. Gervasio, E.I. Ovtchinnikov, and A. Quarteroni. The spectral projection decomposition method for elliptic equations in two dimensions. *SIAM J. Numer. Anal.*, 34(4):1616–1639, 1997.

[34] P. Gervasio and F. Saleri. Stabilized spectral element approximation for the Navier-Stokes equations. *Numerical Methods for Partial Differential Equations*, 14:115–141, 1998.

[35] U. Ghia, K.N. Ghia, and C.T. Shin. High-Re Solutions for Incompressible Flow Using the Navier-Stokes Equations and a Multigrid Method. *J. of Comput. Phys.*, 48:387–411, 1982.

[36] D. Gottlieb and S.A. Orszag. *Numerical Analysis of Spectral Methods: Theory and Applications.* SIAM-CBMS, Philadelphia, 1977.

[37] M.D. Gunzburger. *Finite Element Methods for Viscous Incompressible Flows. A Guide to Theory, Practice and Algorithms.* Academic Press, San Diego, 1989.

[38] P. Haldenwang, G. Labrosse, S. Abboudi, and M. Deville. An element-by-element solution algorithm for problems of structural and solid mechanics. *Comput. Meth. Appl. Mech. Engrg.*, 36:241–254, 1983.

[39] T.J.R. Hughes, L.P. Franca, and M. Balestra. A new finite element formulation for computational fluid dynamics: VII. The Stokes problem with various well-posed boundary conditions: Symmetric formulations that converge for all velocity/pressure spaces. *Comput. Meth. Appl. Mech. Engrg.*, 59:85–99, 1986.

[40] Jr. J. Douglas and J. Wang. An absolutely stabilized finite element method for the Stokes problem. *Math. Comput.*, 52:495–508, 1989.

[41] J. Van Kan. A second-order accurate pressure-correction scheme for viscous incompressible flow. *SIAM J. Sci. Stat. Comput.*, 7(3):870–891, 1986.

[42] G.E. Karniadakis, M. Israeli, and S.A. Orszag. High order splitting methods for the incompressible Navier-Stokes equations. *J. Comput. Phys.*, 97:414–443, 1991.

[43] K.Z. Korczak and A.T. Patera. An isoparametric spectral element method for solution of the Navier-Stokes equations in complex geometries. *J. Comput. Phys.*, 62:361, 1986.

[44] H.O. Kreiss and J. Oliger. Stability of the Fourier method. *SIAM J. Numer. Anal.*, 16:421–433, 1979.

[45] D.N. Ku, D.P. Giddens, C.Z. Zarins, and S. Glagov. Pulsatile flow and atherosclerosis in the human carotid bifurcation. *Arteriosclerosis*, 5:293–302, 1985.

[46] V.I. Lebedev and V.I. Agoshkov. Generalized Schwarz algorithms with variable parameters. Technical report, Report n. 19, Dept. Num. Math., USSR Accademy of Science, 1981. Moscow, (in Russian).

[47] J. L. Lions and E. Magenes. *Nonhomogeneous Boundary Value Problems and Applications*. Springer Verlag, Berlin, 1972.

[48] P.L. Lions. On the Schwarz alternating method III: a variant for nonoverlapping subdomains. In J. Perieaux T.F. Chan, R. Glowinski and O.B. Widlund, editors, *Domain Decomposition Methods for Partial Differential Equations*, pages 202–231, Philadelphia, 1990. SIAM.

[49] Y. Maday, C. Mavripilis, and A.T. Patera. Nonconforming mortar element methods: application to spectral discretizations. In J.Perieaux T.F.Chan, R.Glowinski and O.B.Widlund, editors, *Second International Conference on Domain Decomposition Methods for Partial Differential Equations*, Philadelphia, 1988. SIAM.

[50] Y. Maday, D. Meiron, A.T. Patera, and E.H. Rønquist. Analysis of iterative methods for the steady and unsteady Stokes problem: application to spectral element discretizations. *SIAM J. Sci. Comput.*, 14:310–337, 1993.

[51] Y. Maday and A.T. Patera. Spectral element methods for the incompressible Navier-Stokes equations. In *State-of-the-Art Surveys on Computational Mechanics*. A.K. Noor and J. T. Oden, 1989.

[52] Y. Maday, A.T. Patera, and E.H. Rønquist. An operator-integration-factor splitting method for time-dependent problems: application to incompressible fluid flow. *J. Sci. Comput.*, 5:263–292, 1990.

[53] P.S. Marcus. Simulation of Taylor-Couette flow. Part 1. Numerical methods and comparison with experiments. *J. Fluid Mech.*, 146:45–64, 1984.

[54] L.D. Marini and A. Quarteroni. A relaxation procedure for domain decomposition methods using finite elements. *Numer.Math.*, 55:575–598, 1989.

[55] S.G. Mikhlin and Kh. L. Smolitskii. Approximate Methods for Solving Differential and Integral Equations. *Nauka*, 1965. (In Russian).

[56] Y. Morchoisne. Inhomogeneous flow calculation by spectral methods: monodomain and multidomain techniques. In *Spectral Methods for P.D.E.* R.G. Voight, D. Gottlieb and M.Y. Hussaini, Philadelphia, 1984.

[57] S.A. Orszag and L.C. Kells. Transition to turbolence in plane Pouseuille flow and plane Couette flow. *J. Fluid Mech.*, 96:159–205, 1980.

[58] E. Ovtchinnikov. The construction of a well-conditioned basis for the projection decomposition method. *CALCOLO*, 30(3):255–271, 1993.

[59] E.I. Ovtchinnikov. Projection decomposition method with a well- conditioned basis for the generalised Stokes problem. In *Numerical Methods for Fluid Dynamics V*, pages 515–521, Oxford, 1995. Clarendon Press.

[60] S.S. Pahl. *Schwarz type domain decomposition methods for spectral element discretizations.* PhD thesis, University of the Witwatersand, 1993.

[61] F. Pasquarelli and A. Quarteroni. Effective spectral approximations to convection-diffusion equations. *Comput. Meth. Appl. Mech. Engrg.*, 116:39–51, 1994.

[62] A.T. Patera. A spectral element method for fluid dynamics: laminar flow in a channel expansion. *J. Comput. Phys.*, 54:468–488, 1984.

[63] L. Pavarino. *Domain decomposition methods for the p-version finite element method for elliptic problems.* PhD thesis, Courant Institute of Mathematical Sciences, Department of Mathematics, 1992.

[64] L. Pavarino. Some Schwarz algorithms for the $p-$version finite element method. In A. Quarteroni, J. Perieaux, Y.A. Kuznetsov, and O.B. Widlund, editors, *Sixth International Symposium on Domain Decomposition Methods for Partial Differential Equations*, volume 157, pages 113–119. Contemporary Mathematics, 1994.

[65] K. Perktold, M. Resch, and H. Florian. Pulsatile non-newtonian flow characteristic in a three-dimensional human carotid bifurcation model. *Journal of Biomechanical Engineering, Transactions of the ASME*, 113:464–475, 1991.

[66] A. Pinelli, A. Vacca, and A. Quarteroni. A spectral multidomain method for the numerical simulation of turbulent flows. *J. Comput. Phys.*, 136(2):546–558, 1997.

[67] A. Quarteroni. Domain decomposition algorithms for the Stokes equations. In *Domain Decomposition Methods*, pages 431–442, Philadelphia, 1989. SIAM.

[68] A. Quarteroni and G. Sacchi Landriani. Domain decomposition preconditioners for the spectral collocation methods. *J. Sci. Comput.*, 3:45–75, (1988).

[69] A. Quarteroni and G. Sacchi Landriani. Parallel algorithms for the capacitance matrix method in domain decompositions. *Calcolo*, 25(1-2):75–102, (1988).

[70] A. Quarteroni and A. Valli. Theory and application of Steklov-Poincaré operators for boundary-value problems. In R. Spigler, editor, *Applied and Industrial Mathematics*, pages 179–203, Kluwer Academic Publisher, Dordest, 1990.

[71] A. Quarteroni and A. Valli. *Numerical Approximation of Partial Differential Equations*. Springer Verlag, Heidelberg, 1994.

[72] A. Quarteroni and A. Valli. *Domain Decomposition Methods for Partial Differential Equations*. Oxford University Press, Oxford, 1998.

[73] A. Quarteroni and E. Zampieri. Finite element preconditioning for Legendre spectral collocation approximation to elliptic equations and systems. *SIAM J. Numer. Anal.*, 29:917–936, 1992.

[74] R. Rannacher. On Chorin's projection method for the incompressible Navier-Stokes equations. In R. Rautmann J.G. Heywood, K. Masuda and S.A. Slonnikov, editors, *The Navier-Stokes Equations II: Theory and Numerical Methods*, pages 167–183. Springer-Verlag, Berlin, 1992.

[75] D. Schötzau, K. Gerdes, and C. Schwab. Galerkin least squares $hp-$FEM for the Stokes problem. *C.R.A.S., Paris*, 326(Serie I):249–254, 1998.

[76] C. Schwab and M. Suri. Mixed $hp-$FEM for Stokes and non-Newtonian flow. to appear in Comp. Meth. Appl. Mech. Engrg., 1998.

[77] J. Shen. On error estimates of the projection methods for the Navier Stokes equations: second order schemes. *Math. Comp.*, 65(215):1039–1065, 1997.

[78] S.J. Sherwin and G.E. Karniadakis. A triangular spectral element method; applications to the incompressible Navier-Stokes equations. *Comp. Meth. Appl. Mech. Engrg.*, 123:189–229, 1995.

[79] J.C. Simo and F. Armero. Unconditional stability and long-term behaviour of transient algorithms for the incompressible Navier-Stokes and Euler equations. *Comp. Meth. Appl. Mech. Engrg.*, 111:111–154, 1992.

[80] B.F. Smith. *Domain decomposition algorithms for the partial differential equations of linear elasticity*. PhD thesis, Courant Institute of Mathematical Science, 1990.

[81] B.F. Smith. A domain decomposition algorithm for elliptic problems in three dimensions. *SIAM J. Sci. Comput.*, 13(1):219–234, 1992.

[82] E. Zampieri. A multidomain spectral collocation solver for the elasticity problem. In D. E. Keyes, T.F.Chan, G.Meurant, J.S. Scroggs, and R.G. Voigt, editors, *Fifth International Symposium on Domain Decomposition Methods for Partial Differential Equations*, pages 614–623, Philadelphia, 1992. SIAM.